AD

USAAMRDL TECHNICAL REPORT 71-39

ADVANCED TECHNOLOGY V/STOL PROPELLER RETENTION SYSTEM INVESTIGATION

By

E. M. Varholak

January 1972

EUSTIS DIRECTORATE
U. S. ARMY AIR MOBILITY RESEARCH AND DEVELOPMENT LABORATORY
FORT EUSTIS, VIRGINIA

CONTRACT DAAJ02-70-C-0030
HAMILTON STANDARD
DIVISION OF UNITED AIRCRAFT CORPORATION
WINDSOR LOCKS, CONNECTICUT

71

DISCLAIMERS

The findings in this report are not to be construed as an official Department of the Army position unless so designated by other authorized documents.

When Government drawings, specifications, or other data are used for any purpose other than in connection with a definitely related Government procurement operation, the United States Government thereby incurs no responsibility nor any obligation whatsoever; and the fact that the Government may have formulated, furnished, or in any way supplied the said drawings, specifications, or other data is not to be regarded by implication or otherwise as in any manner licensing the holder or any other person or corporation, or conveying any rights or permission, to manufacture, use, or sell any patented invention that may in any way be related thereto.

Trade names cited in this report do not constitute an official endorsement or approval of the use of such commercial hardware or software.

DISPOSITION INSTRUCTIONS

Destroy this report when no longer needed. Do not return it to the originator.

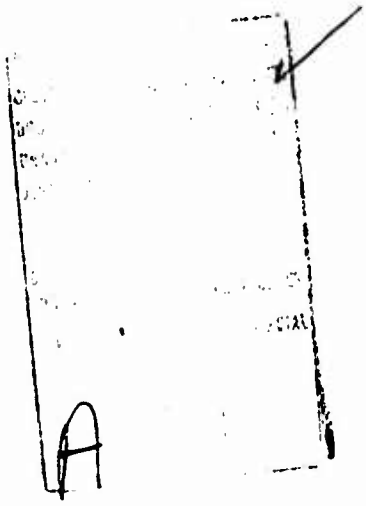

DEPARTMENT OF THE ARMY
U. S. ARMY AIR MOBILITY RESEARCH & DEVELOPMENT LABORATORY
EUSTIS DIRECTORATE
FORT EUSTIS, VIRGINIA 23604

This report was prepared by Hamilton Standard, Division of United Aircraft Corporation, under the terms of Contract DAAJ02-70-C-0030. The technical monitor for this contract was Mr. James Gomez, Propulsion Division.

The objective of this program was to investigate the feasibility of using a boron-aluminum composite structure for an advanced V/STOL propeller blade spar/retention, principally by performing fatigue testing.

The basic design concept used for the one-half scale retention system was confirmed by fatigue tests, with the retention specimen failing above the ultimate load conditions considered.

Unclassified

Security Classification

DOCUMENT CONTROL DATA - R & D

(Security classification of title, body of abstract and indexing annotation must be entered when the overall report is classified)

1. ORIGINATING ACTIVITY *(Corporate author)*

Hamilton Standard
Division of United Aircraft Corporation
Windsor Locks, Connecticut

2a. REPORT SECURITY CLASSIFICATION

Unclassified

2b. GROUP

3. REPORT TITLE

ADVANCED TECHNOLOGY V/STOL PROPELLER RETENTION SYSTEM INVESTIGATION

4. DESCRIPTIVE NOTES *(Type of report and inclusive dates)*

Final Report

5. AUTHOR(S) *(First name, middle initial, last name)*

Edward M. Varholak

6. REPORT DATE	7a. TOTAL NO. OF PAGES	7b. NO. OF REFS
January 1972	71	2

8a. CONTRACT OR GRANT NO.	9a. ORIGINATOR'S REPORT NUMBER(S)
DAAJ02-70-C-0030	
b. PROJECT NO.	USAAMRDL Technical Report 71-39
c. Task 1G162203D14415	9b. OTHER REPORT NO(S) *(Any other numbers that may be assigned this report)*
d.	

10. DISTRIBUTION STATEMENT

Approved for public release; distribution unlimited.

11. SUPPLEMENTARY NOTES	12. SPONSORING MILITARY ACTIVITY
Details of illustrations in this document may be better studied on microfiche	Eustis Directorate U.S. Army Air Mobility R&D Laboratory Fort Eustis, Virginia

13. ABSTRACT

The objective of this program was to investigate the feasibility of employing a BORSIC®/Aluminum composite structure for a propeller blade retention for an advanced-technology, 2000-shp, V/STOL propeller system.

This was accomplished by the design of a one-half scale composite retention system, the fabrication of three test elements, and the fatigue test of this system, which is compatible with the 33LF propeller.

The basic design concept employed for this system was confirmed, with the retention failing above the ultimate load conditions considered.

DD FORM 1 NOV 68 1473 REPLACES DD FORM 1473, 1 JAN 64, WHICH IS OBSOLETE FOR ARMY USE.

Unclassified

Security Classification

14. KEY WORDS	LINK A		LINK B		LINK C	
	ROLE	WT	ROLE	WT	ROLE	WT
BORSIC® Fiber reinforced metal matrix material Fatigue test V/STOL propeller system						

Task 1G162203D14415
Contract DAAJ02-70-C-0030
USAAMRDL Technical Report 71-39
January 1972

ADVANCED TECHNOLOGY V/STOL PROPELLER RETENTION SYSTEM INVESTIGATION

Final Report

By

E. M. Varholak

Prepared by

Hamilton Standard
Division of United Aircraft Corporation
Windsor Locks, Connecticut

for

EUSTIS DIRECTORATE
U. S. ARMY AIR MOBILITY RESEARCH AND DEVELOPMENT LABORATORY
FORT EUSTIS, VIRGINIA

SUMMARY

The objective of this program was to investigate the feasibility of employing a BORSIC®/Aluminum composite structure for a propeller blade retention for an advanced-technology, 2000-shp, V/STOL propeller system.

This was accomplished by the design of a one-half scale composite retention system, the fabrication of three test elements, and the fatigue test of this system, which is compatible with the 33LF propeller.

The basic design concept employed for this system was confirmed, with the retention failing above the ultimate load conditions considered.

FOREWORD

The preparation of this final report concluded a 12-month exploratory development program conducted by Hamilton Standard under Contract DAAJ02-70-C-0030, Task 1G162203D14415. This program was an outgrowth of previous contracts with USAAMRDL (Contracts DAAJ02-67-C-0073 and DAAJ02-68-C-0079) which involved feasibility studies of "Advanced Technology V/STOL Propeller".

The work associated with this program served to strengthen the technological background for a composite retention concept for employment in an advanced V/STOL propeller system.

Under the cognizance of R. F. Wilson, Program Manager, Advanced Composites, this program was initially directed by W. J. Fisher, Assistant Project Engineer, and completed by E. M. Varholak, Senior Experimental Engineer, under the supervision of L. Stoltze, Assistant Project Engineer. Significant contributions were made by the following Hamilton Standard technical personnel:

Design Studies	Mr. E. Luiz	Design Engineer
	Mr. D. Crombie	Senior Experimental Engineer
BORSIC/Aluminum Blade Retention Manufacture	Mr. G. Kutner	Assistant Project Engineer
	Mr. A. Olson	Experimental Engineer
Testing	Mr. J. Mattavi	Senior Test Engineer
	Mr. S. Cohen	Analytical Engineer
	Mr. R. Walters	Senior Experimental Engineer

TABLE OF CONTENTS

LIST OF ILLUSTRATIONS

LIST OF SYMBOLS

CF	centrifugal load, lb
ESA	experimental stress analysis
FBF	preceeded by number indicates distance from butt face of retention
FSI	fatigue strength investigation
Hz	cycles per second
I/C	section modulus of spar
IN	inside surface of spar
M	bending moment
OOP	out of plane
OUT	outer surface of spar
R_{ac}	axial retention reaction due to centrifugal load
R_{am}	axial retention reaction due to moment load
R_{at}	total axial retention reaction
R_{rc}	radial retention reaction due to centrifugal load
R_{rm}	radial retention reaction due to moment load
R_{rt}	total radial retention reaction
1P	once per revolution spar bending load
3P	three times per revolution spar bending load
σ	tensile or compressive stress, psi

INTRODUCTION

It is recognized throughout the aviation community that the future of V/STOL aircraft is dependent upon further advances in the state of the art for lightweight subsystems which will reflect improvements in cost and mission effectiveness of the systems.

The U. S. Army, in mid 1967, awarded a study contract to Hamilton Standard to investigate the application of advanced materials and design concepts to the next generation of V/STOL propellers. This effort produced advanced technology propeller design concepts which are significantly lighter than current V/STOL propellers.

Propeller blades represent approximately 35 percent of the total weight of today's advanced propeller gearbox systems. The blade sets the design loads for such major components as the barrel, actuator, gearbox, and support structure. This represents the single most determining factor on the total system weight. Therefore, in seeking to define the maximum weight reduction potential for the 1970 - 1975 propeller system, prime attention must be directed toward blade weight reduction. This requires a detailed evaluation of composite blade structures to best utilize the advanced material properties.

The initial step in the development of an aluminum matrix boron composite retention was taken under Contract DAAJ02-68-C-0079, in which Hamilton Standard designed, fabricated, and tensile tested two reduced-size boron/aluminum retention designs.

The design study produced two retention concepts.

The first design consisted of a conical spar section with a uniform wall thickness of BORSIC/Aluminum. The inboard end of the spar was enveloped internally and externally by aluminum subcomponents to produce the retention portion of the spar. The axial load is transmitted into the composite by shear at the composite-aluminum braze joint plus compression which is a result of the wedging action of the two aluminum subcomponents on the spar.

The second design was identical to the first design concept dimensionally; however, it differed in the manner in which the load was distributed within the retention. The boron/aluminum material was separated into three layers by aluminum wedges within the retention.

The tensile test results revealed the superiority of the first design over the second design. The wedges of the latter design caused the load to be distributed unevenly among the three segments of the composite wall. The first design performed well, with the strength value obtained being characteristic of specimen data of that period.

The encouraging results of this initial phase in the development of a boron/aluminum retention lead to the acquisition of fatigue data on this system. The propeller blade spar is usually sized by the fatigue strength of the retention and therefore establishes the determination of retention fatigue strength as an important step toward the ultimate goal: investigation of a full-size boron/aluminum spar by exploratory development.

Efforts of this program were directed toward acquiring fatigue data on the composite retention system, reduced in size but compatible to a known production propeller system.

BORSIC/ALUMINUM BLADE RETENTION INVESTIGATION

The feasibility of employing an advanced composite material in the construction of a known production propeller blade retention system was continued under this program. Efforts to accomplish this objective consisted of the design of a retention system similar to that tested under a previous contract (DAAJ02-68-C-0079), the fabrication of four BORSIC/Aluminum retention specimens, and the fatigue test of three of these specimens in a 33LF barrel system to verify the established design parameters.

RETENTION DESIGN

The spar and retention system was designed to operate in the 33LF barrel with loading as imposed on the Aero-Commander propeller system. The design technique is based on test results obtained previously under Contract DAAJ02-68-C-0079, USAAVLABS Technical Report 69-59.

The actual loads considered in the design were 31,500 pounds centrifugal load and 3,000 in.-lb 1P out-of-plane bending moment. The design analysis was carried out primarily by use of the computer program for Thin Shells of Revolution (H088). This program is capable of handling a multilayered orthotropic material which makes it ideal for use with composite spars. The loads must be inputted to the program in the form of Fourier harmonics.

The centrifugal load is reacted at the retention by an axial and a radial load transferred through the ball bearing. The axial load reaction to the centrifugal load is shown in Figure 1 as R_{ac}. This is a load which is assumed to be uniform around the entire circumference of the ball race and is measured in pounds per inch. The radial load reaction is shown in Figure 1 as R_{rc} and is also assumed to be uniform around the circumference of the ball race.

The moment loading is reacted at the retention by an axial and radial load also. These reactions are shown in Figure 2 as R_{am} for the axial component and R_{rm} for the radial component. In order to maintain force balance of the system, on one side of the retention the moment reactions must be positive and on the opposite side they must be negative. Since there is no connection between the barrel and the retention other than a ball bearing, which cannot impart a tension load, the positive reaction to the centrifugal loads in the axial and radial directions must be large enough so that the negative reactions of the bending load do not cause the

net reactions, R_{at} and R_{rt}, to become negative. Figure 3 shows the net reactions to the bending and centrifugal loads imposed.

The load distribution for the bending moment can be approximated by a combination of zero, second, and fourth harmonics in the radial direction and by a first harmonic in the axial direction. These load distributions are shown in Figures 4 and 5 .

The allowable stress levels used for the design are given in Table I. The allowable stress levels in shear are used for matrix, interlaminar bond, and braze joint strengths. Using the shear allowables noted, the spar and retention system were designed to withstand a minimum of 10 million cycles of 1P out-of-plane bending at 3000 in.-lb and a steady centrifugal load of 31,500 lb.

The stresses calculated in the spar and retention for the loads and load distribution of Figures 1, 2, 3, 4 and 5 are shown in Figures 6, 7 and 8. Figure 6 shows the axial stress due to centrifugal loads as calculated by computer program H088. The discontinuities in the curve are due to the method of sectioning of the spar for input into the computer. The large discontinuities shown near the ball race station (approximately one inch from the butt face of the spar) are due to the influence of the applied loads on the retention by the ball. Figure 7 shows the bending stress calculated in the spar by H088 for a 3000 in.-lb moment. Figure 8 shows the shear stress due to bending moments only, which is calculated for the spar by H088. The shear stress due to axial loading must be added to the bending to obtain the maximum stress in shear. The shear stress due to axial loading was calculated by a computer program for calculating shear at tab endings. The tab ending or, in our case, the end of the outer aluminum retention member is the most critical area for shear stress because of the sudden section change in the retention. The computer program gives a value of approximately 400 psi for the stress at the retention end. This stress is at a point four inches from the butt face of the spar. The shear stresses may now be plotted on a Goodman diagram by using the shear calculated for bending as a cyclic stress and the shear stress due to centrifugal load as a steady or mean stress. Figure 9 shows this plot. The point represented in Figure 9 by the square symbol was obtained by using a stress concentration factor of 1. A stress concentration value of 3, calculated for a homogeneous material, was employed for this investigation,and the point is represented in Figure 9 by the circular symbol. Using the stress concentration factor of 3, the stress is 70% of maximum allowable cyclic stress for 10^7 cycles. A stress concentration factor of 4 could be

TABLE I. DESIGN ALLOWABLE STRESSES BORSIC/AL COMPOSITE		
Stress	Tensile (psi)	Fatigue (psi)
Axial	100,000	30,000
Transverse	10,000	3,000
Shear	10,000	1,800

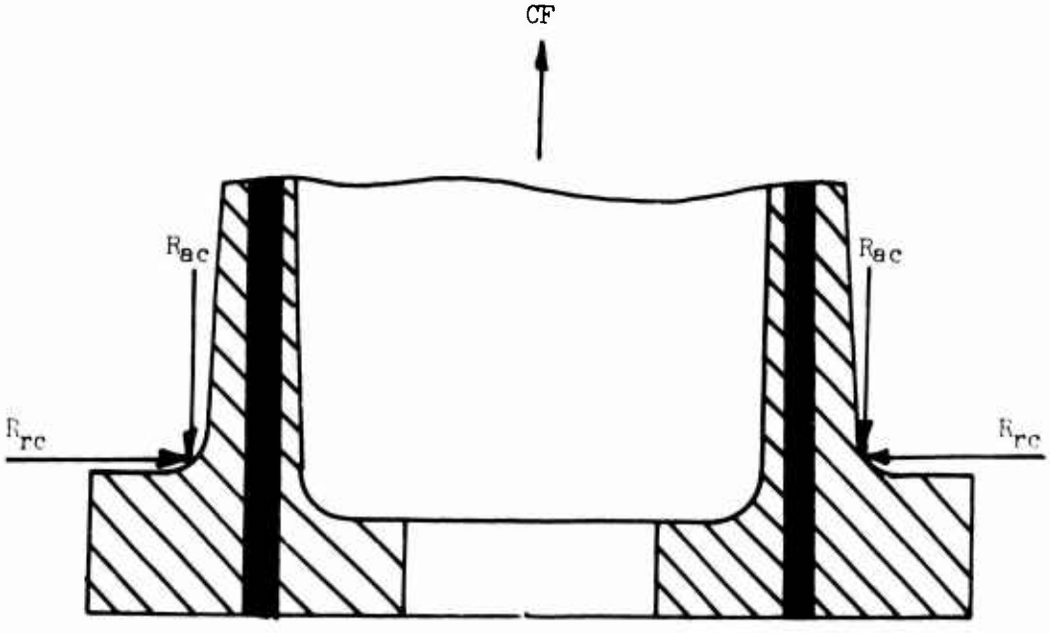

Figure 1. Free Body of Retention Reactions to Centrifugal Load.

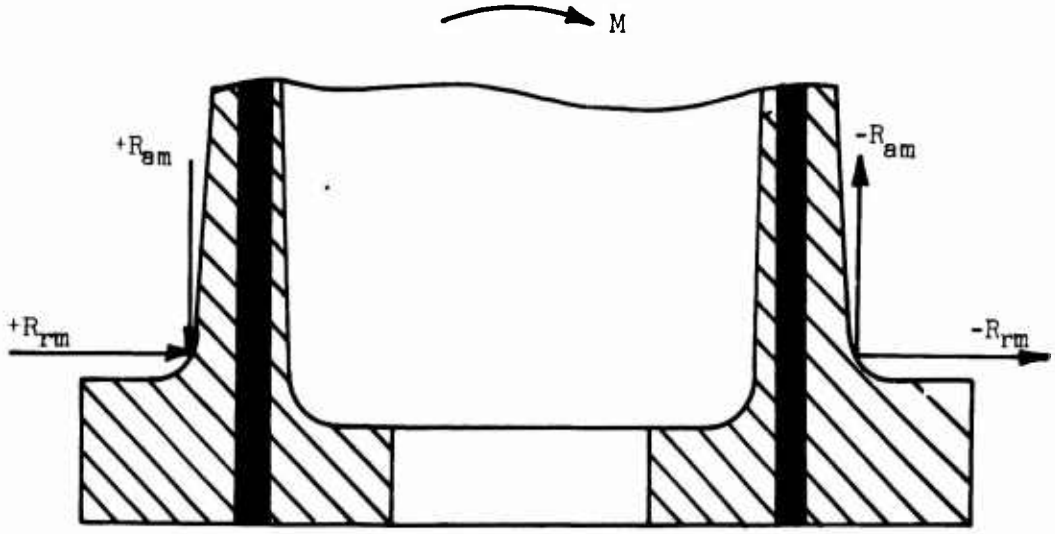

Figure 2. Free Body of Retention Reactions to Moment Load.

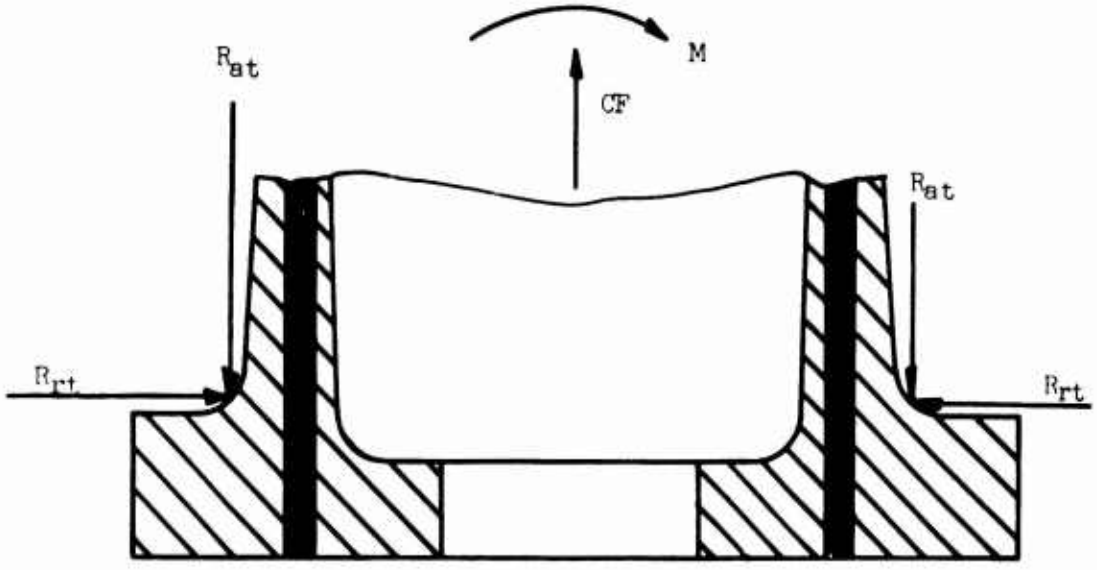

Figure 3. Free Body of Retention Reactions to Combined Load.

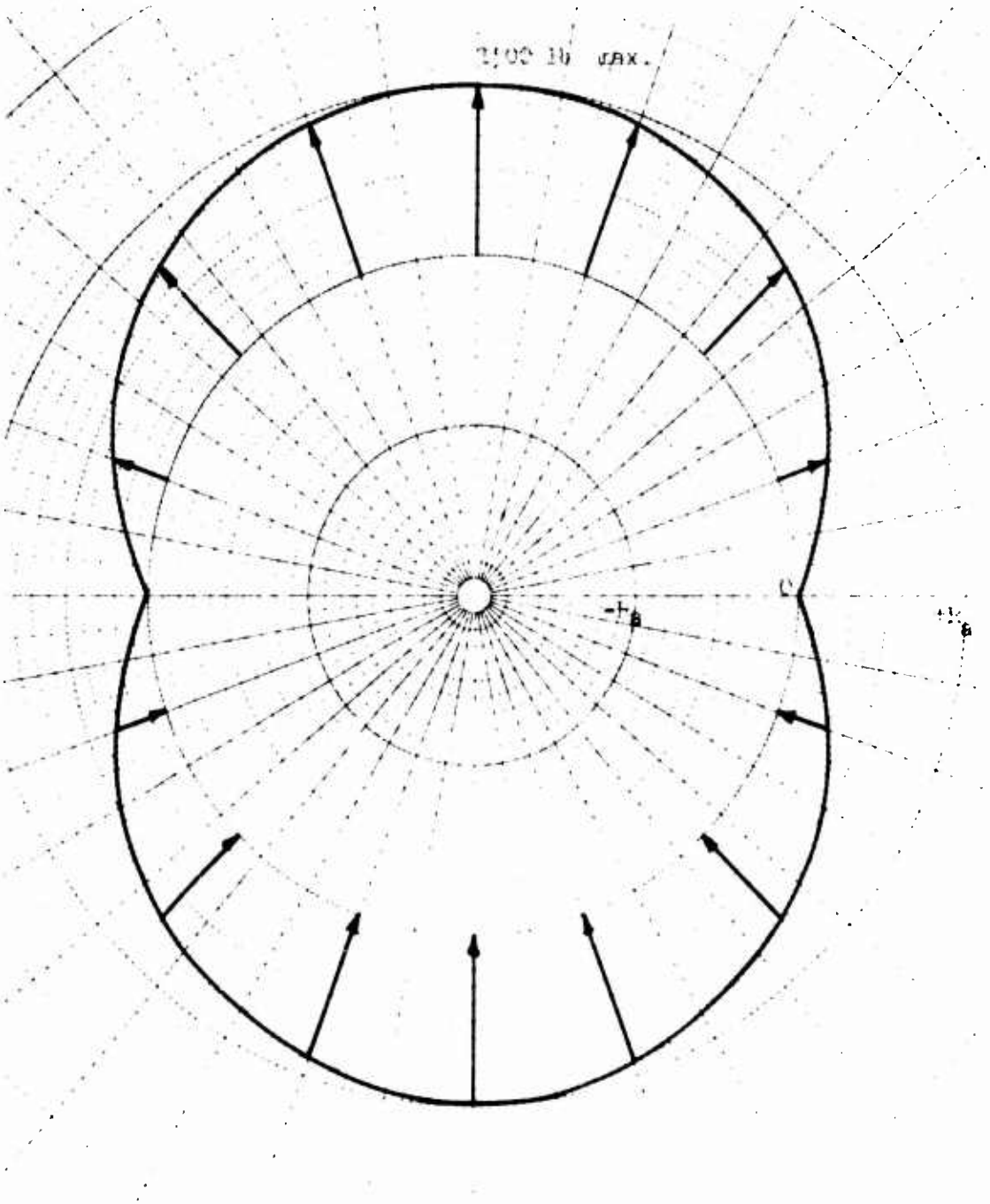

Figure 4. Axial Load Distribution Due to Moment Load.

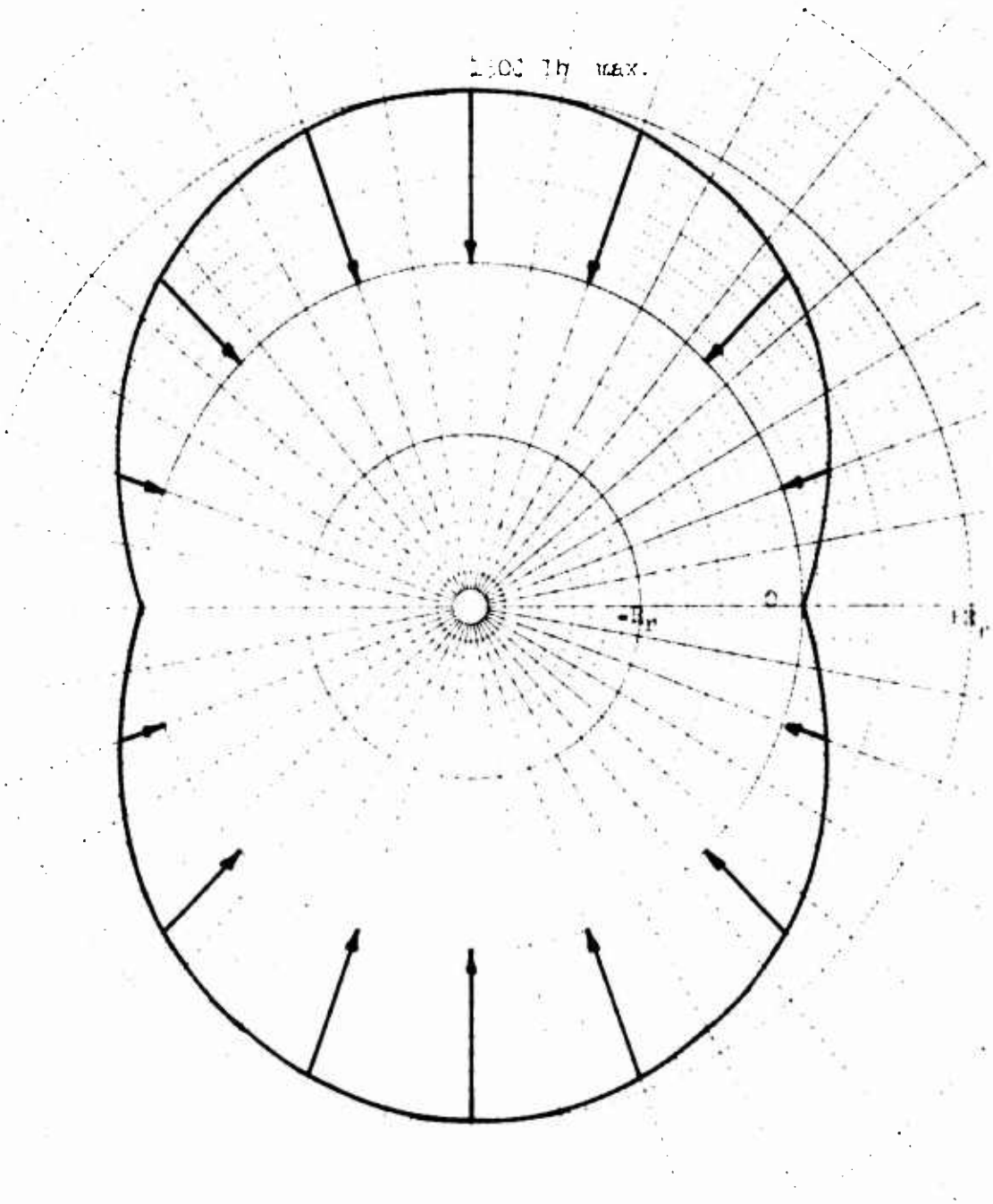

Figure 5. Radial Load Distribution Due to Moment Load.

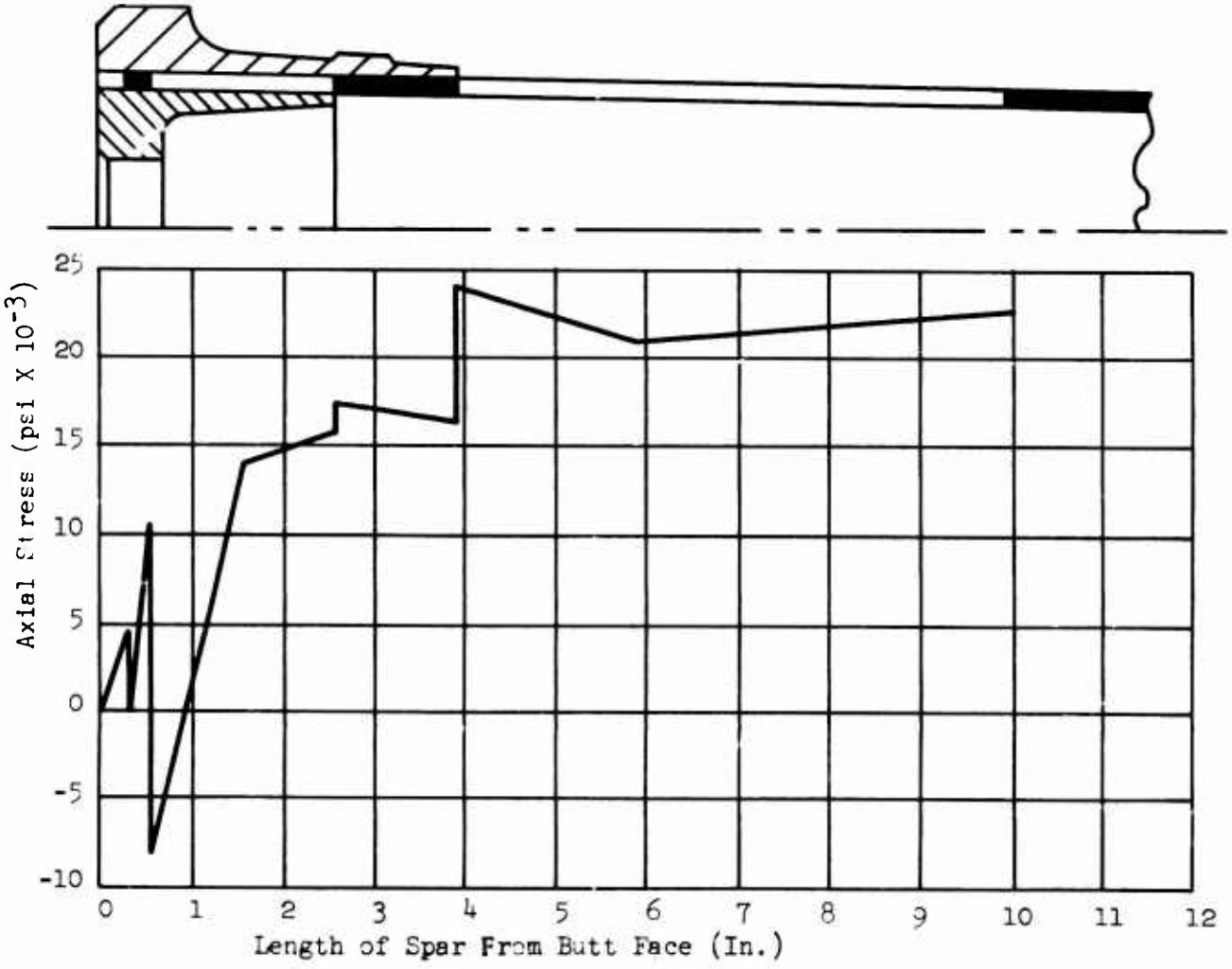

Figure 6. Calculated Axial Stress Due to Centrifugal Load.

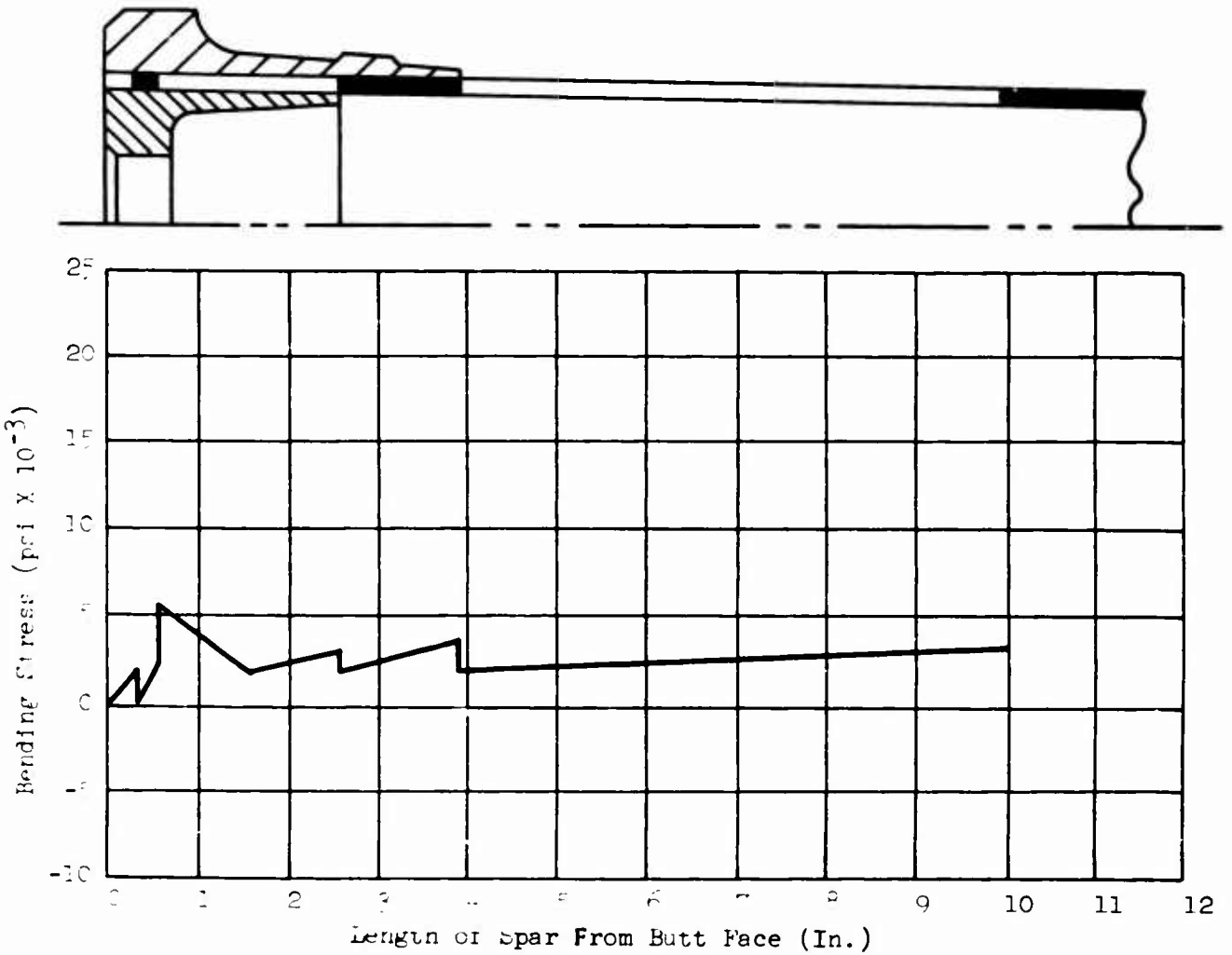

Figure 7. Calculated Bending Stress Due to Moment Load.

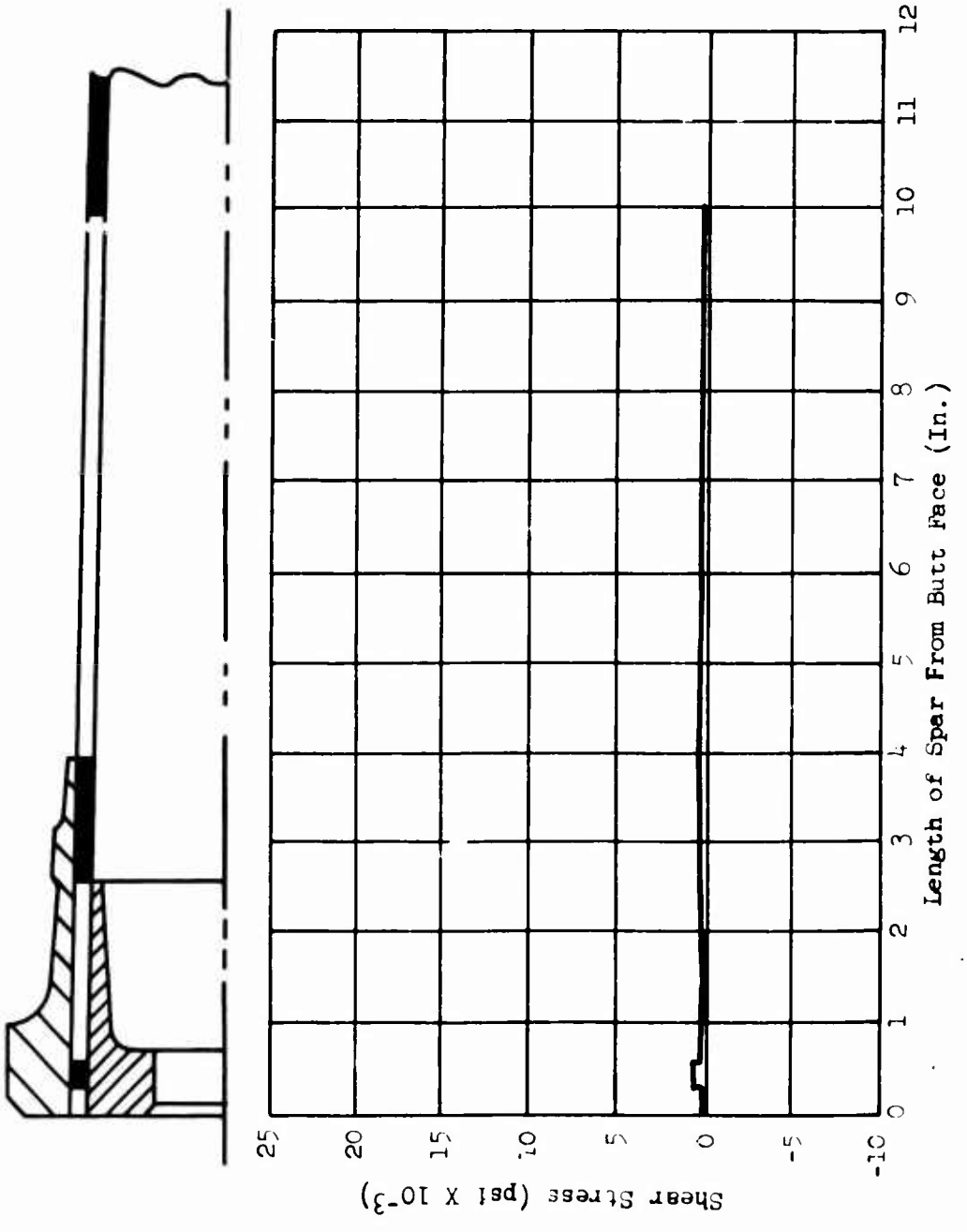

Figure 8. Calculated Shear Stress Due to Moment Load.

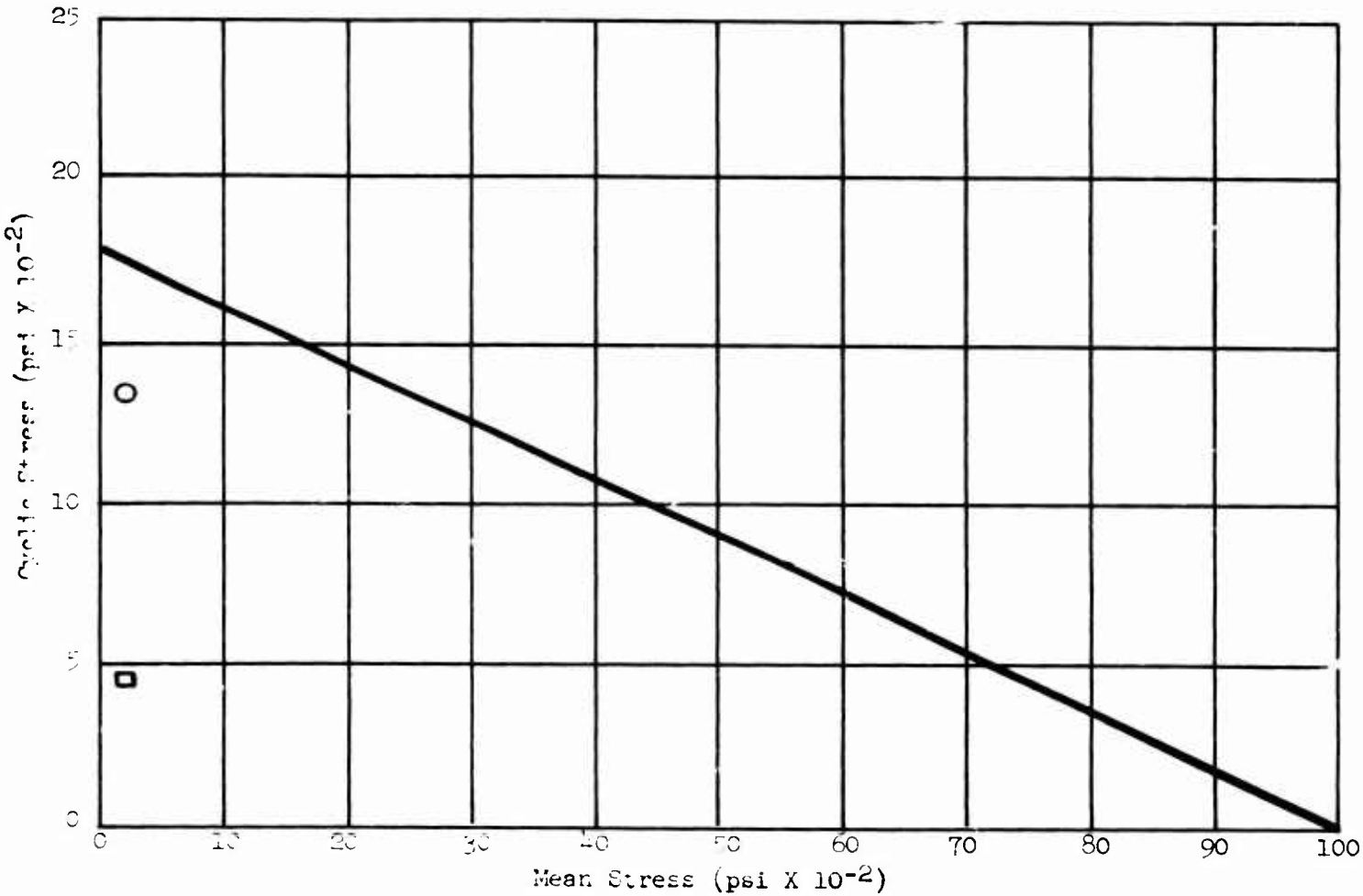

Figure 9. Goodman Diagram for 10^7 Cycles Shear Loading.

assumed in the most conservative case to account for any unknown behavior of the orthotropic material actually being used; in such a case, the stress would be 92% of maximum allowable cyclic. In either case, the design should then be good for the cycles required at the loads specified.

RETENTION FABRICATION

Tape Fabrication

The composite portion of the retention assembly is composed of 30 layers of a metal matrix foil tape reinforced with a silicon-coated boron fiber, designated BORSIC. The individual tape layer employed as the basic building block in composite structures is considered the best form for manufacturing operation. The single-ply tape is a mechanically stable structure by virtue of the fixed fiber position uniformly spaced within the tape. The tape form permits ease of handling and may be readily positioned on dies without disturbing the integrity of the fiber spacing. In addition, the single-ply tape can be easily cut or punched.

The incorporation of the fiber and metal matrix material into a monolayer tape is accomplished in three basic operations:

1. Mandrel preparation and substrate layup
2. Filament winding of the fiber
3. Plasma spraying of the 6061 aluminum onto the fiber and substrate

The equipment employed during these operations consists of large winding drums, approximately 40 inches in diameter. The mandrels are cut at one face and held in place by tension springs. This joint serves as an expansion joint and an area for fiber splicing and tape cutting for removal of the finished tape from the drum. Lengths of 10 feet by 15 inches wide are now obtainable.

The aluminum braze substrate, Alcoa 713, with a nominal thickness of 0.001 inch, is placed around the drum with care to prevent the foil from wrinkling. The foil is held in place by tape at the expansion joint of the drum.

The drum is then placed in the lathe-like winder and the filament winding initiated. The fibers are wound at 175 turns/inch. The drum is then placed on the plasma spray equipment. The matrix material, 6061, is applied by injecting the aluminum powder into

the plasma gun. The powder unites with the hot argon gas of the plasma arc, liquifying in the exothermic or recombination zone of the gun, and is impacted and quickly solidified on the fiber and substrate. See Figure 10. The fiber represents approximately 50% of the tape weight.

Spar Fabrication

Fabrication of the composite spar section is essentially a manual operation with the consolidation phase being the only exception. Care is exercised through these operations to minimize contamination of the part. Clean white gloves are utilized during the initial preparation and layup phases, with the consolidation of the part being performed in a vacuum.

The tape is initially cut into rectangular shaped pieces, and then each rectangle is cut into two pieces, with the length larger than the test piece and one width equal to one-fourth the circumference of the base of the conical specimen and the other one-fourth that of the tip circumference. See Figure 11. Both sections are then placed on a wooden mandrel; one section is rotated and tack brazed into position as illustrated in Figure 12.

This operation eliminates the possibility of the part being misoriented during the following buildup of layers. The entire procedure is then repeated by butting successive pieces and forming them tightly to the surface of the mandrel.

The sections are dimensionally changed as required to compensate for the diameter increases which result as each layer is added. The direction of rotation of each section is reversed, and the butt joints are staggered relative to the location of the joint in the preceding layers to maintain a balanced fiber alignment.

Each individual tape layer is wiped with gauze and an acetone cleaning solvent prior to the layup operation.

Thirty layers of composite tape were assembled for each conical section which, after consolidation, yielded a specimen with a 0.150-inch wall and a fiber volume of approximately 48%.

The unconsolidated tape assembly was placed in the spar braze rig, as shown in Figures 13 and 14, for the bonding and compaction operation. This is accomplished by removing the assembly from the wooden mandrel and placing it onto the metallic inner mandrel. The outer die is set in place over the composite cone and bolted

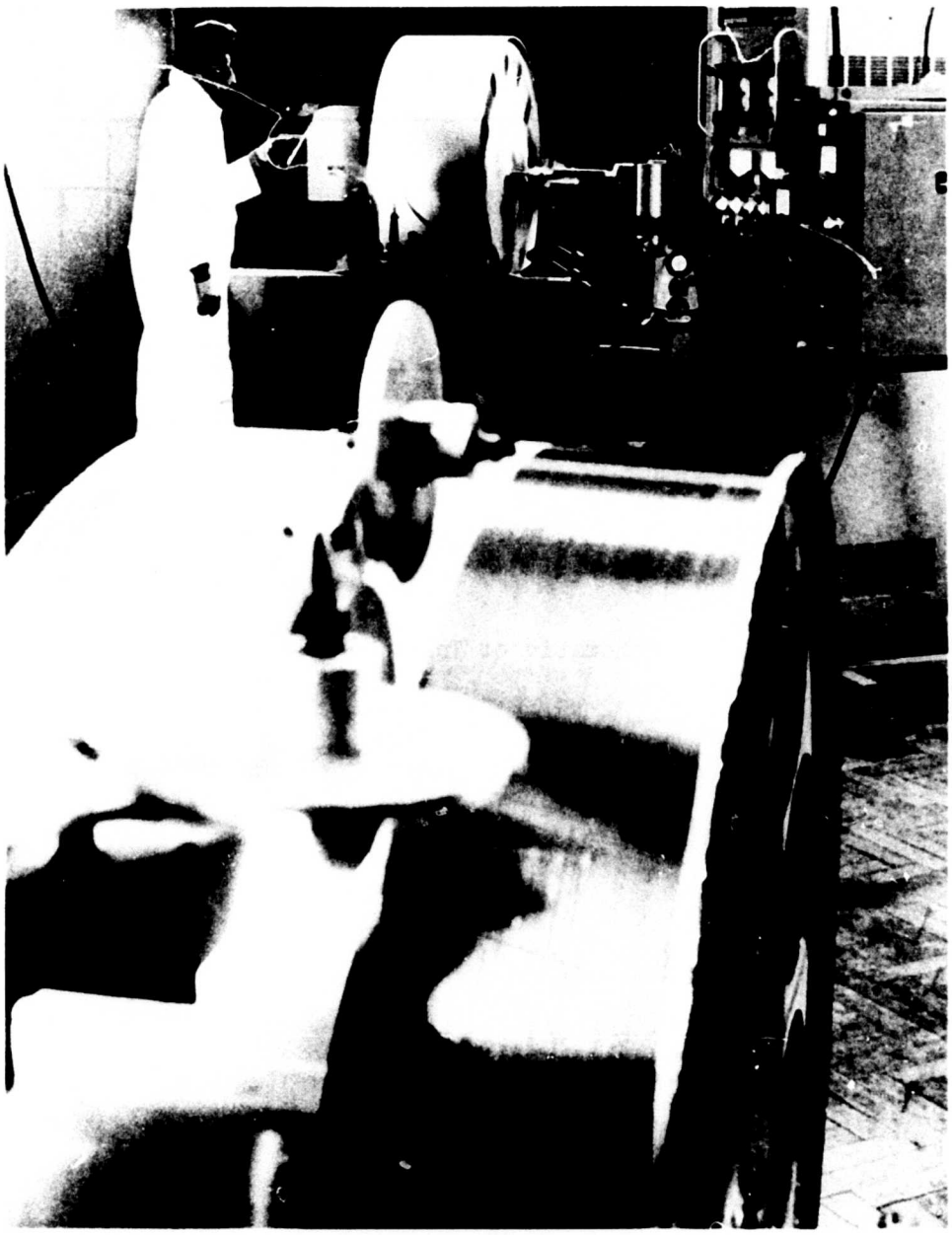

Figure 10. Tape Manufacturing Setup.

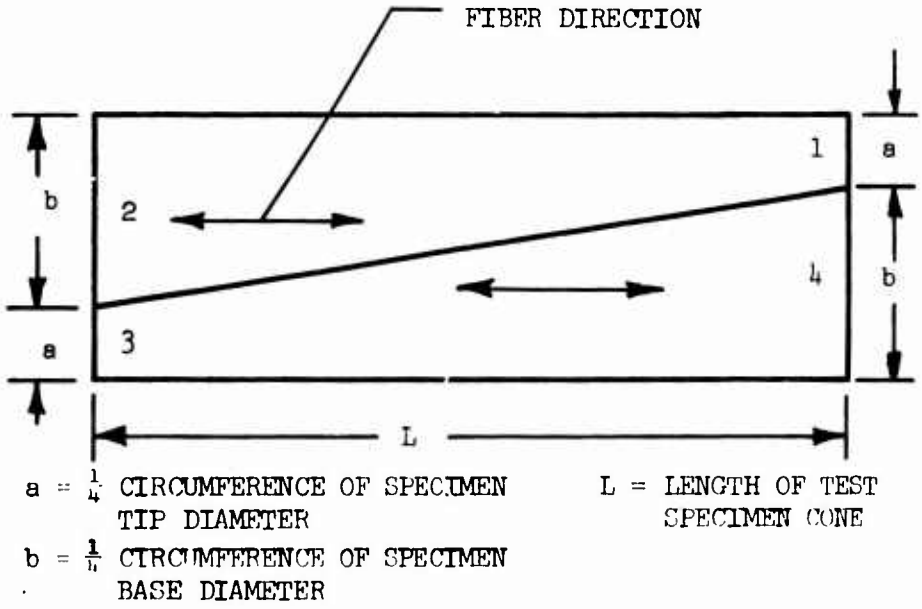

Figure 11. Schematic of Tape-Cutting Operation.

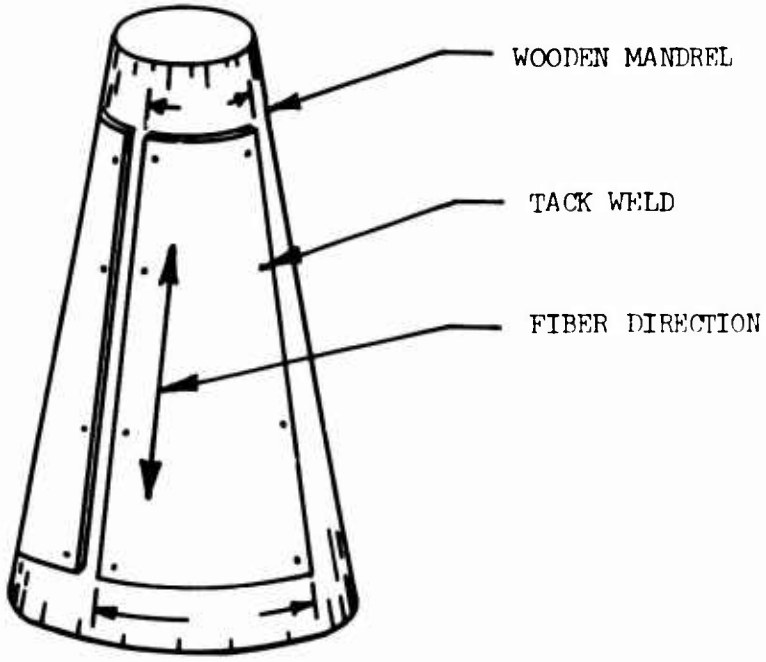

Figure 12. Tape Layup Operation.

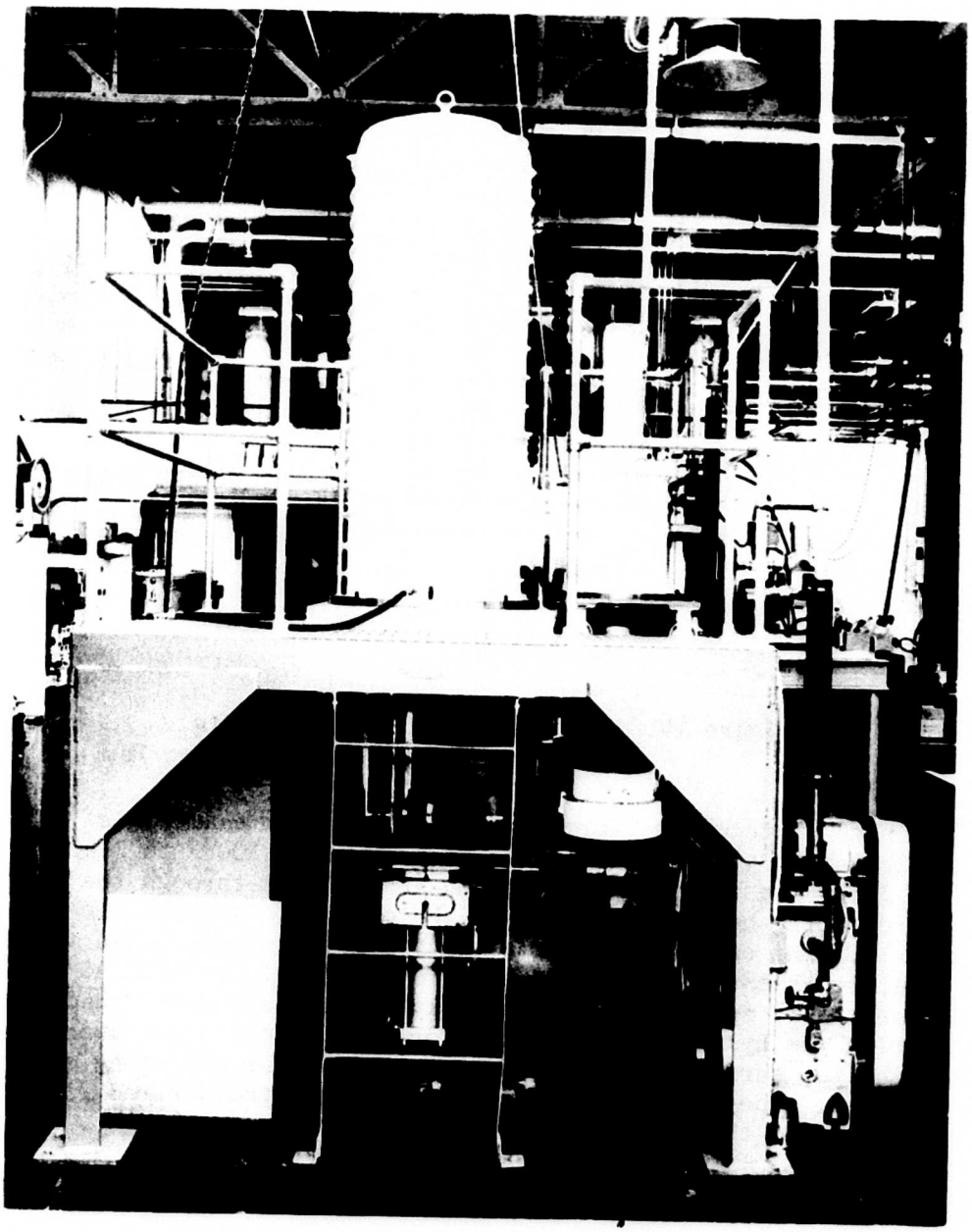

Figure 13. Spar Braze Rig.

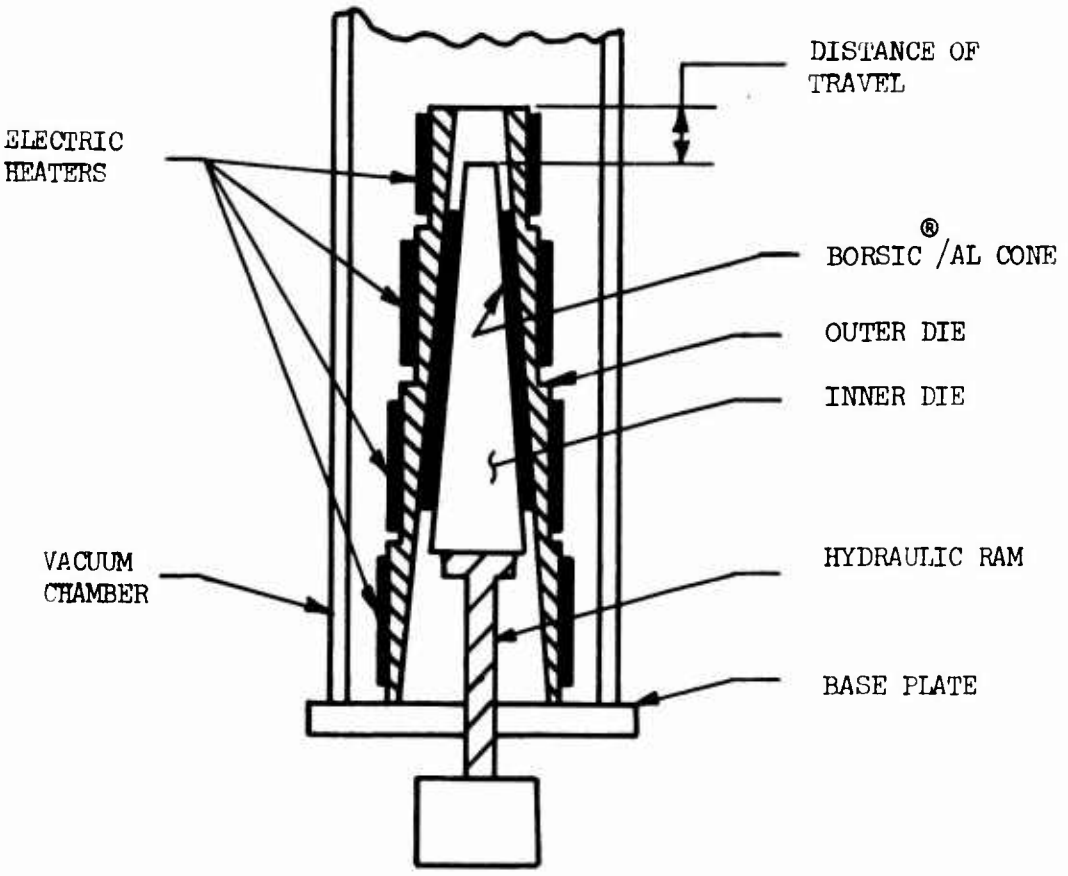

Figure 14. Schematic of Spar Braze Rig Showing Heaters and Hydraulic Ram.

to the base plate of the forming rig. The vacuum chamber is installed and a vacuum drawn. The temperature, 1100°F to 1140°F, required for the braze-bond operation is acquired through the use of electric heaters attached to the outer die as shown in Figure 15. The composite material is finally compacted when the material reaches the designated temperature of 1100°F to 1140°F, and pressure is applied to the assembly. This is accomplished by activating the hydraulic ram, which forces the inner die upward until the top surfaces of both the inner and outer retaining die are aligned. The dies were designed to produce the desired final dimensions when this condition is reached.

Retention Component Assembly

The second major process is attaching the aluminum components to the composite spar to complete the retention end of the

composite specimen. These components, which envelop the composite spar at the external and internal surfaces, were machined prior to assembly of the members. The internal aluminum component was completely finish machined, whereas the outer member was roughed out with only the internal surfaces being finished. The outer surfaces of the latter component are completed to finished dimensions after braze-bonding, as shown in Figure 16.

The surfaces of the components were cleaned prior to assembly. The braze foil and composite surfaces were wiped with acetone, whereas the aluminum surfaces were scoured with Gibson Cleaner and flushed with water until a water-break-free surface was attained. All parts were then dried.

All components are brazed in one operation. Both aluminum components are carefully prefitted to the BORSIC/Aluminum spar, removed and reassembled with braze foil, Alcoa 718, installed between the component and spar. The inner aluminum support rested on a pedestal positioned at the base of the furnace, with a steel weight added to the aluminum outer block to assure proper positioning of the parts by imparting a preload. The assembly was placed in an ABAR vacuum furnace; see Figure 17. The aluminum braze alloy 718 was employed in the joint because its melting point, 1085° to 1100°F, is below the melting range of the consolidated spar.

The entire assembly was then heated to 1085°F - 1100°F in a vacuum of 0.3×10^{-3} torr maximum. The part was allowed to cool slowly to room temperature prior to removal from the furnace.

The entire assembly was then heat treated to establish a T6 condition in the aluminum components. The specimens were heated to 920°F for 3 hours, warm water quenched, aged at 350°F for 8 to 10 hours and slow cooled to room temperature.

Final machining of the retention section of the spar was completed after the heat-treating operation, with all surfaces being shot peened to harden them. Photographs of the finished specimen are shown in Figure 18.

Fatigue Test Specimen Assembly

Additional fixturing was necessary to produce the stresses that the retention would see due to centrifugal loading. A loading mechanism was devised and fabricated and may be seen in Figure 19.

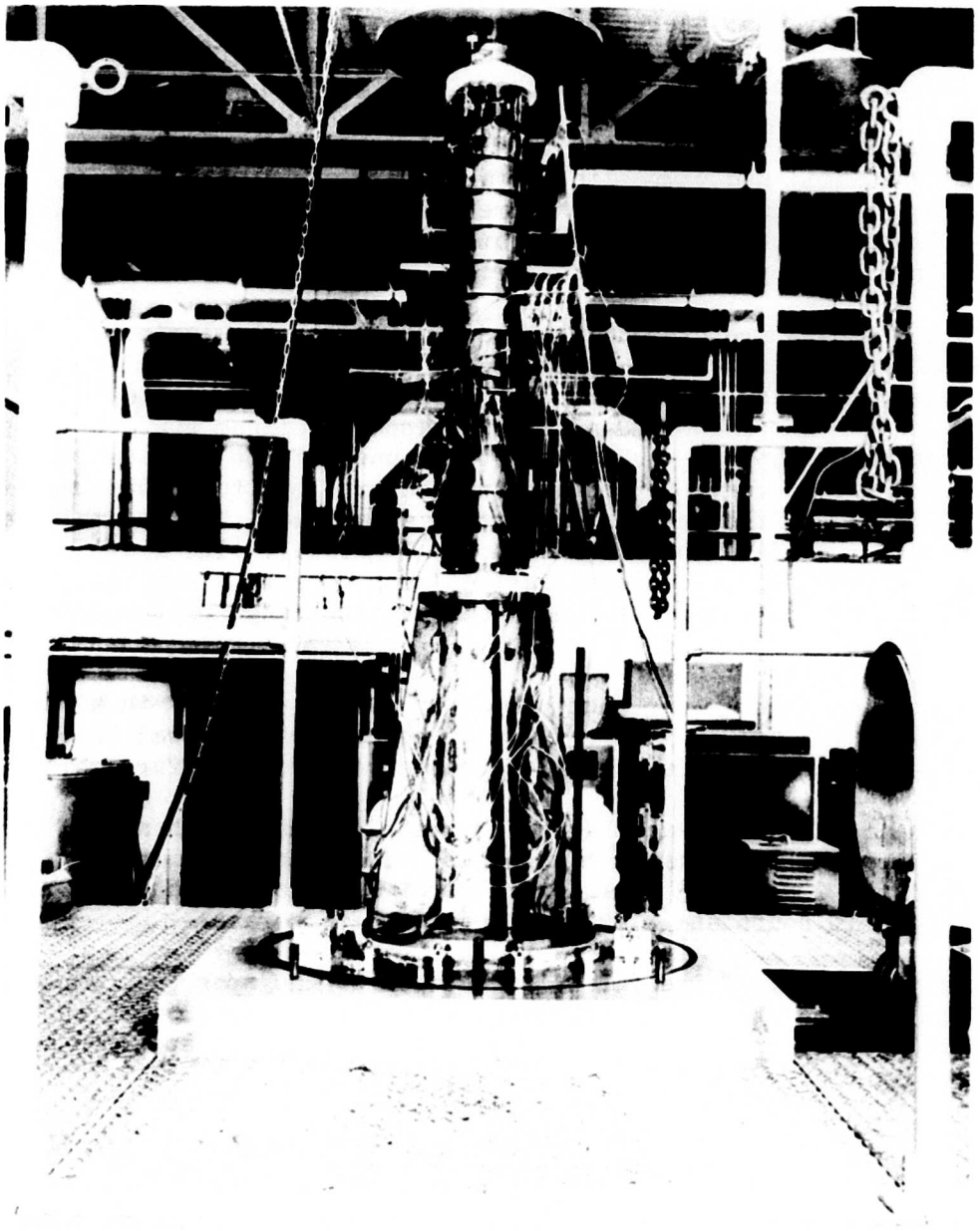

Figure 15. Electric Heaters on Outer Die.

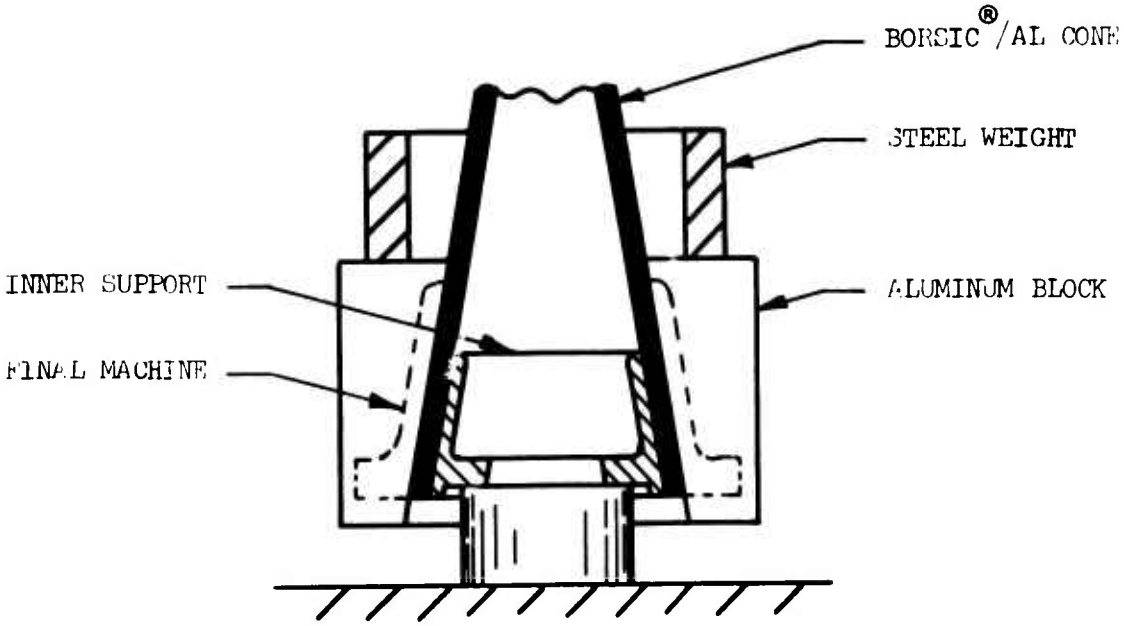

Figure 16. Braze Bond Fixture for Bonding Aluminum Components.

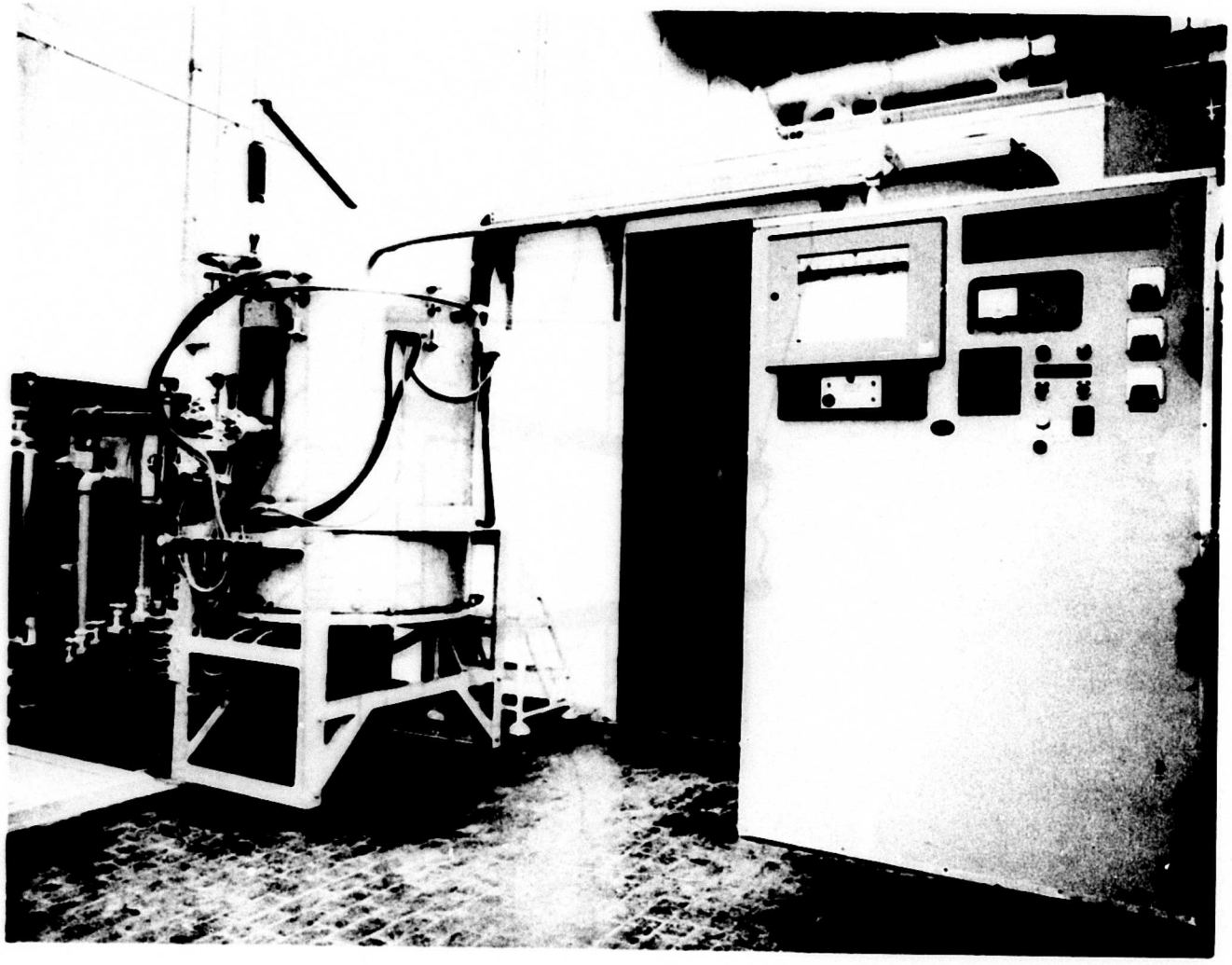

Figure 17. ABAR Vacuum Furnace.

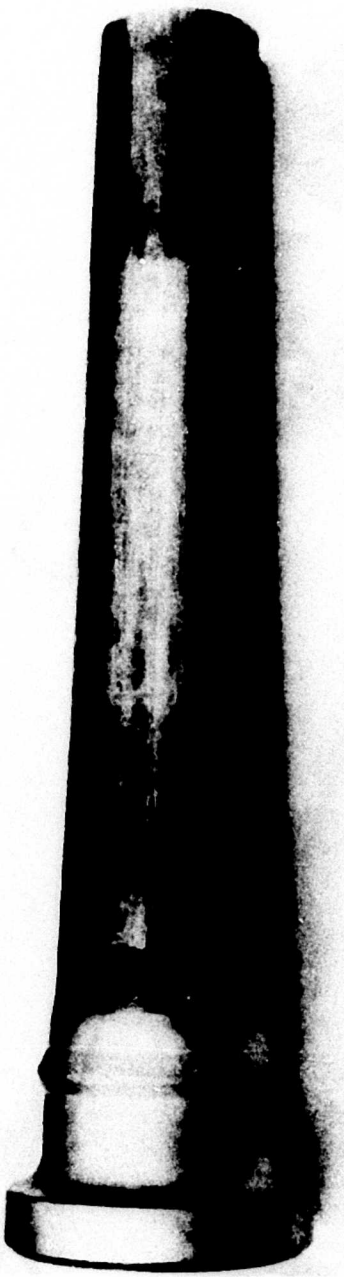

Figure 18. Finished Spar/Retention Specimen.

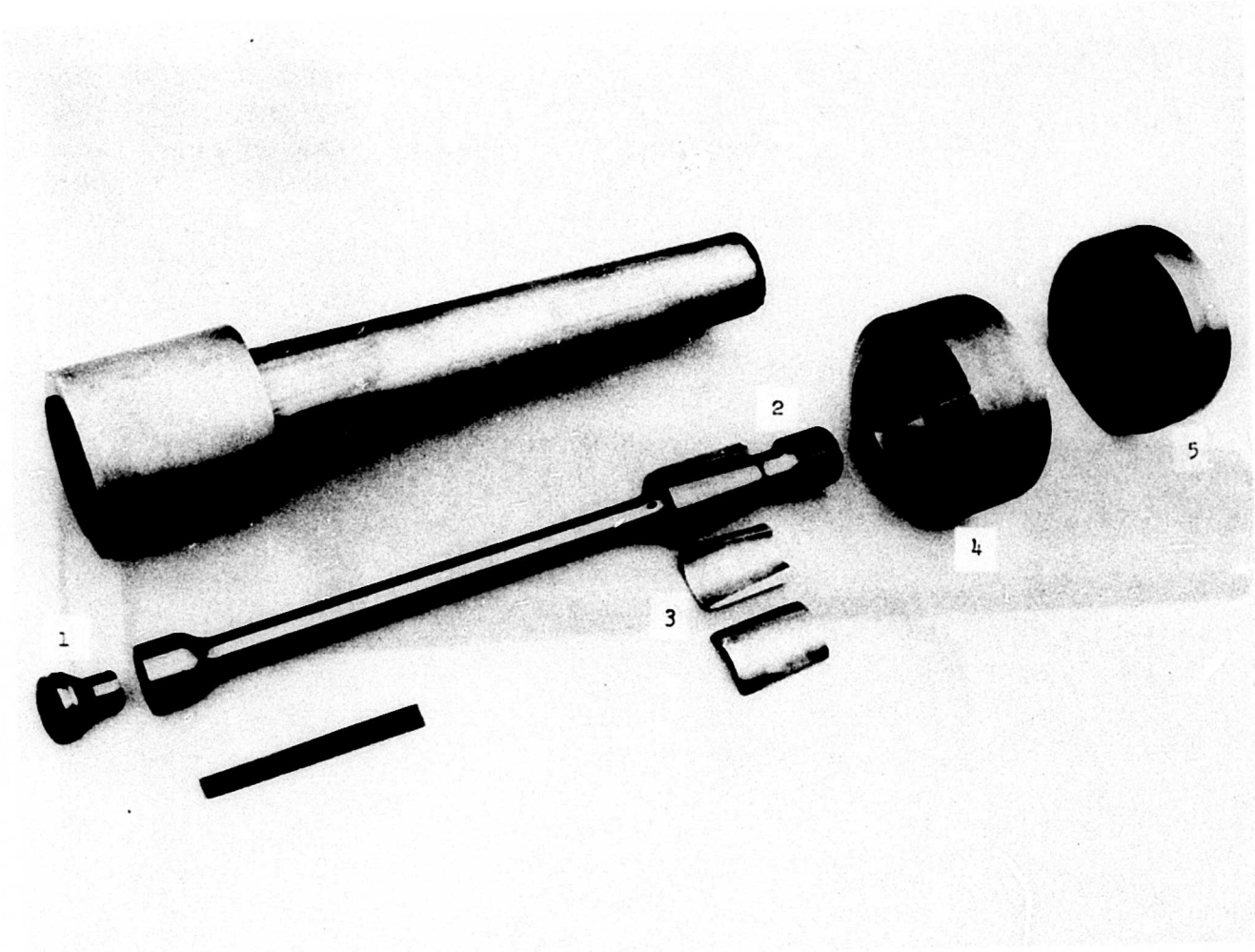

Figure 19. Spar and Centrifugal Preload Bar and Wedges.

The hardware pieces consisted of a preload bar (Item 1), a loading wedge (Item 2), an expansion ring (Item 3), a test spar collar (Item 4) and an expansion ring retainer (Item 5).

The spar collar was adhesively bonded to the outboard external surface of the spar. The loading wedge, Item 2, was then inserted into the cavity of the spar until the thread end emerged at the tip. The expansion ring, Item 3, and three wedge-shape segments were fitted between the loading wedge and the internal surface of the spar. The expansion ring retainer, Item 5, was slipped over the exposed threaded end of the wedge and bolted to the collar, Item 4. A retainer nut was then threaded on to the load bar until contact was made with the ring retainer. The preload bar was then inserted at the inboard end of the specimen, and the specimen was ready for assembly in the barrel. A section of the assembly is shown in Figure 20. The loading wedge reflected in this sketch proved to be incapable of handling the desired load when it began to buckle during the initial static tests. A new bar was designed which has a larger cross-sectional area. The old bar was sectioned so that the outboard loading taper and threads could be used with the new loading bar. The ball joint in the loading bar was then moved outboard so that the joint was between the new load bar and the old loading taper and thread. This provided a loading mechanism with the required stiffness to withstand the preload necessary to impart the 31,500-pound centrifugal load to the spar. Figure 21 shows the redesigned bar and the old loading taper and thread.

RETENTION LABORATORY TEST

The retention design was subjected to an Experimental Stress Analysis (ESA) and a Fatigue Strength Investigation (FSI). The testing was carried out according to the plan of test presented in the Appendix.

The spar and retention were tested in the 33LF barrel. The 33LF designation identifies a barrel which is a model 3, 3 bladed type, with an L shank size, which is flange mounted. The loading was applied by loading bars and wedges as shown in Figure 20. The centrifugal load was generated by a hydraulic ram acting on a tapered center post (Item 1) in the barrel. The taper was forced up against wedges (Item 2) which pushed on the loading bars (Item 3). The loading bars were bottomed on a second set of wedges (Item 4) on the outboard end of the spar which, in turn, transmitted the load into the spar itself. The tapered center post can be locked with a threaded member to retain the preload. The preload was measured by use of strain gages on the loading bars.

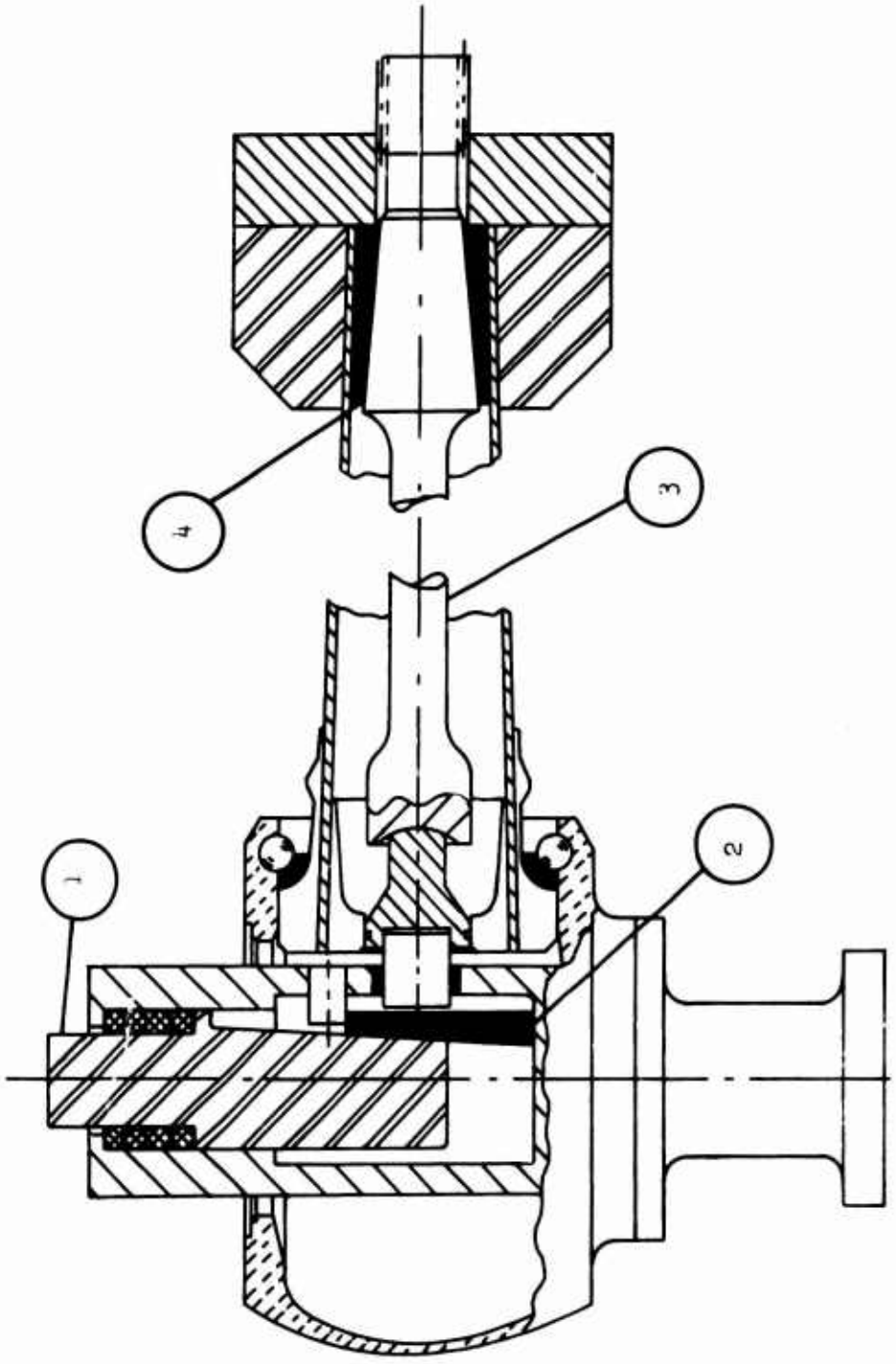

Figure 20. Cross Section of Preload Assembly.

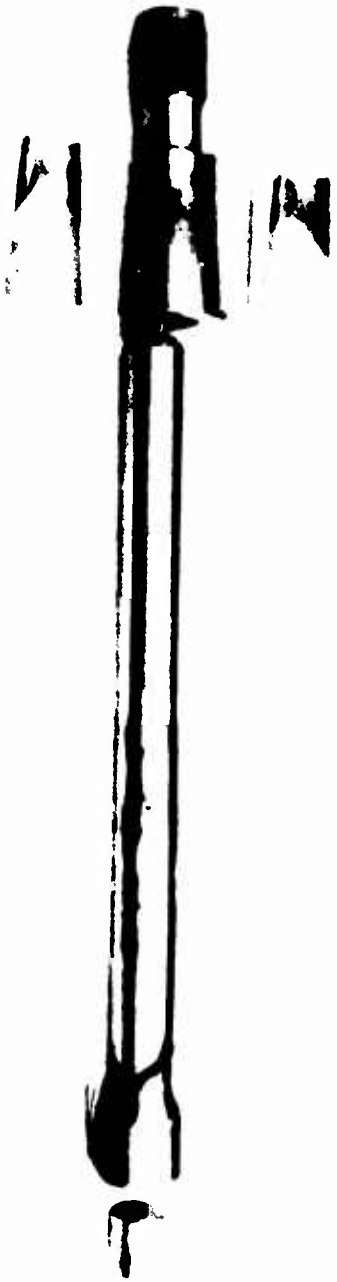

Figure 21. Redesigned Preload Bar.

ESA

During the ESA centrifugal and bending loads were applied to the spars. The centrifugal load was applied in four increments to an average maximum load of 30,900 lb. The loading increments were 7,800 lb, 15,500 lb, 23,500 lb, and 30,900 lb. The loading was done in increments to insure that the behavior of the spar was linear with load before applying the full centrifugal load. The full complement of strain gages were read at each load level. A gage installation is contained in Figure 44 in the Appendix. When the maximum load was achieved it was locked in by means of a threaded collar and the hydraulic pressure was removed. The spar and barrel assembly was then prepared for the bending load application. The bending loads were applied to individual spars on the barrel by means of calibrated spring and cable arrangement which pulls up on the outboard end of the spar in the out-of-plane direction while the barrel is clamped to a fixed base, as shown in Figure 22. The bending loads were applied at three levels corresponding to 50%, 100% and 150% of the design load of 3000 in.-lb. The average maximum moment attained was 4460 in.-lb. The moment was measured at a station 5.5 inches from the test bar butt face. The full complement of strain gages was recorded at each level.

FSI

At the completion of the ESA, the barrel assembly with the centrifugal preload still locked in was mounted on an electromagnetic vibration motor for fatigue testing, (Figure 23). The vibration motor excites the barrel and thus the spars in a 3P-00P mode. That is, each spar vibrates out of the plane of normal propeller rotation at a simulated frequency of 3 times the speed of propeller rotation. The actual frequency of vibration is set at the natural frequency of the barrel and spar combination in the out-of-plane direction. This frequency was chosen because of the low power required to drive the test and because of the rapid accumulation of cycles at this frequency as compared to the actual frequency of a 3P vibration mode in an aircraft. The natural frequency of the spar system as designed was to be 65 Hz and this was the planned frequency of vibration. The actual natural frequency of the unit was 82 Hz and this was the test vibration frequency. The higher frequency was beneficial in that it allowed the test cycles to be accumulated more quickly. Each arm of the barrel assembly was tuned by adding small tip weights to the spar specimens to insure that all arms vibrated at the same resonant frequency. The moment required is applied by setting the vibration motor power to a level which causes the strain gages to match the readings taken during the ESA at a particular bending moment. The first fatigue level of 1500 in.-lb moment was achieved by applying power until the strain

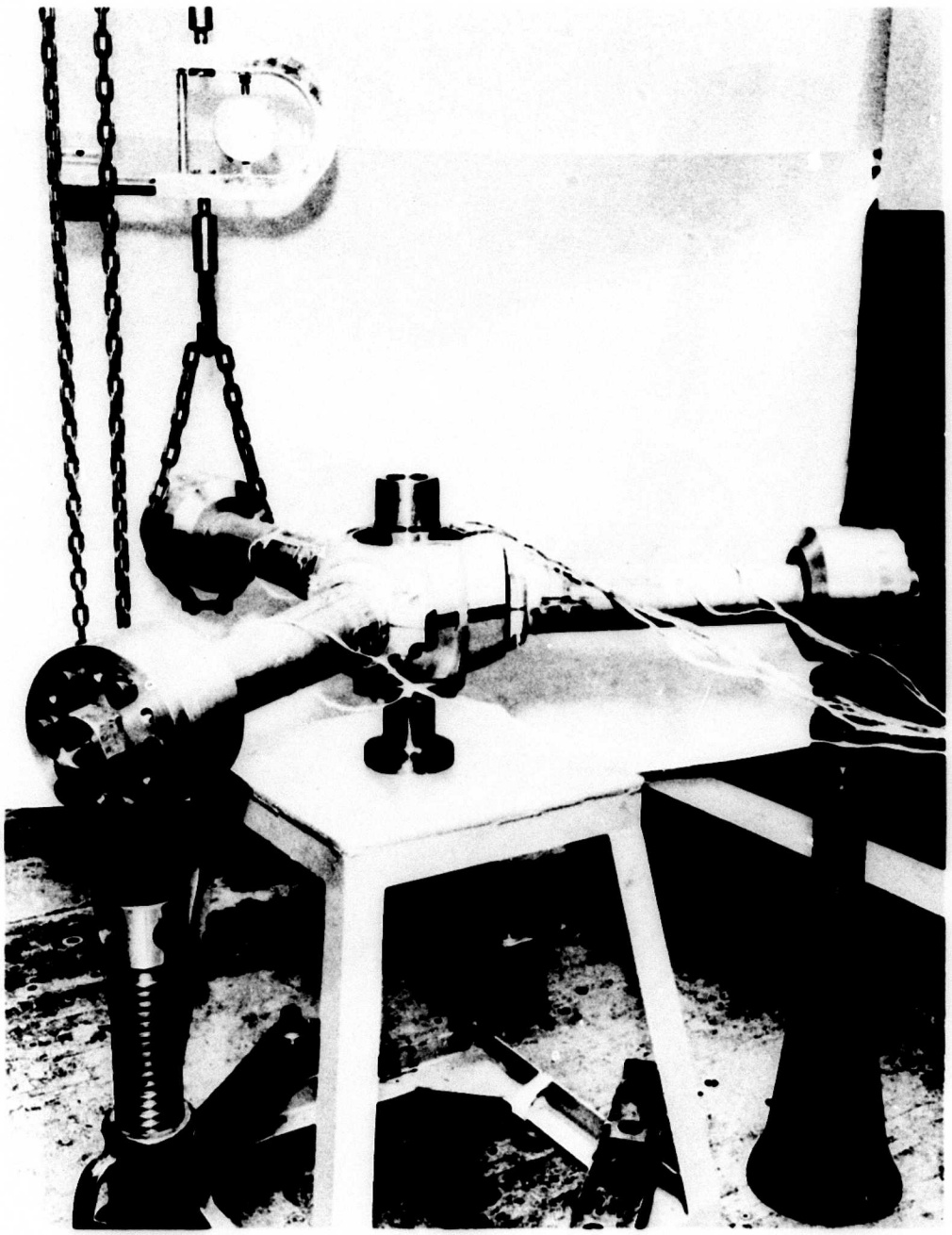

Figure 22. ESA Bending Load Application.

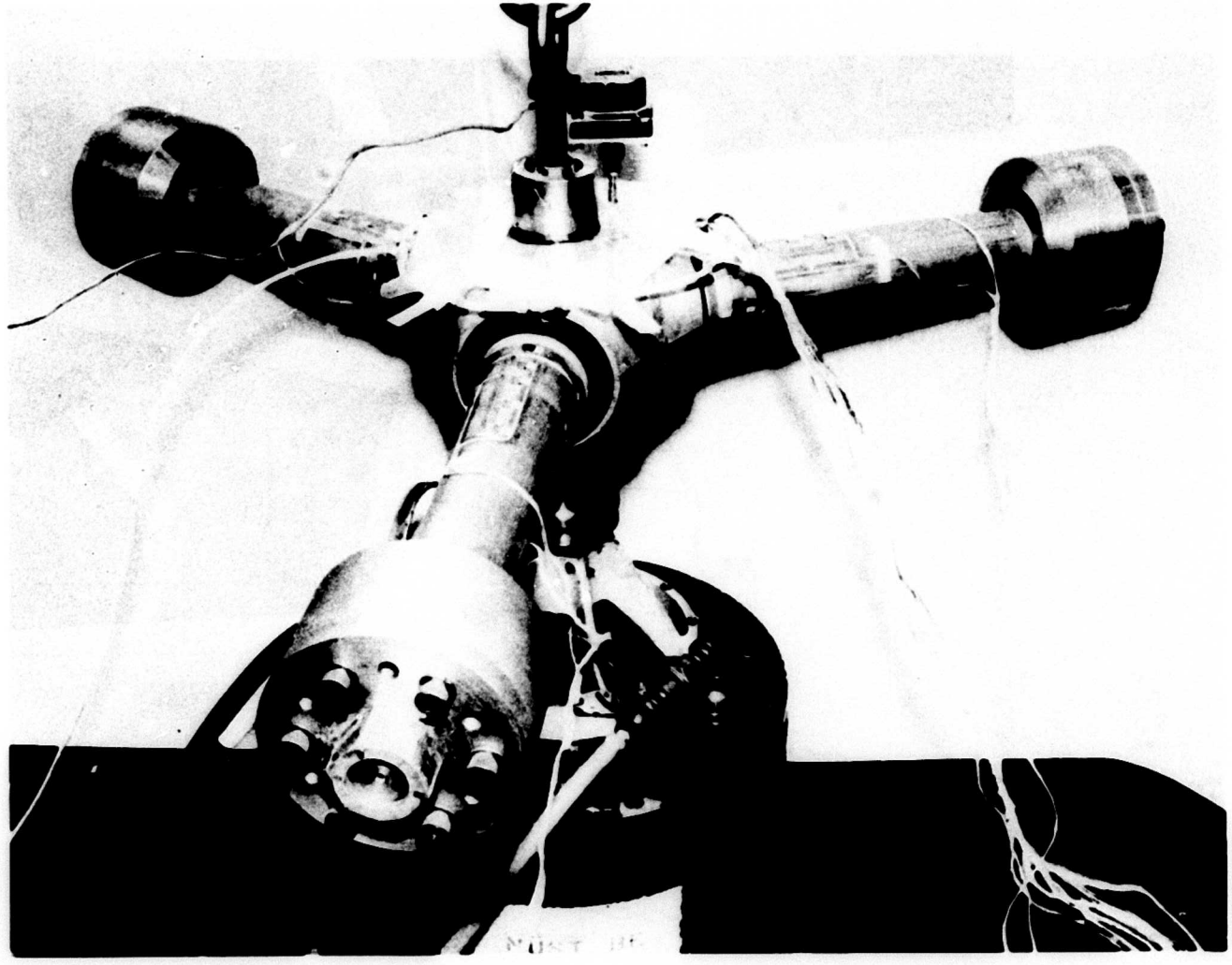

Figure 23. Vibration Motor and Setup for FSI Bending Loads.

gages showed a reading equivalent to the reading shown for 1500 in.-lb on the static test.

During fatigue testing, the frequency and strain gages were checked at 15 minute intervals, since fracture of a test bar would be indicated by a marked difference in frequency or strain gage readings. The frequency was monitored with a Strobocom unit which reads frequency accurate to 3 decimal places. This accuracy allows very close frequency control and acts as an indicator for very small frequency changes which might be caused by the first stages of a fracture.

Test Results

The moment distribution obtained from the ESA for the BORSIC/Aluminum test bars is plotted in Figure 24. A subsequent dynamic calibration revealed no change in the moment distribution at approximately 82 Hz, the test setup resonant frequency. Table II is a summary of the stressing of the BORSIC/Aluminum blade for the four centrifugal loading and three bending moment conditions evaluated. Loading of the barrel under both conditions revealed that strain increased linearly with load. Stressing of the BORSIC/Aluminum blade spar was as predicted, with no evidence of shell action being present. The maximum steady stress recorded at a distance of 5.5 inches from the butt face of the spar due to a centrifugal loading of 30,900 lb was 21,510 psi on the external surface of the spar section and 19,020 psi on the internal surface. The maximum bending stresses recorded at these same locations for a 4,460 in.-lb bending moment at the 5.5-inch station were 4,140 psi on the external surface and 3,650 psi on the internal surface. These values are in good agreement with the stresses predicted by simple beam bending theory, since σ out/ σ in = 1.1 based on the section modulus (I/C) at the 5.5-inch station. The hoop stressing in the spar is approximately 10% of the longitudinal stressing. The above results indicate that there was no secondary bending present, and that the structural behavior of the spar was predictable.

The composite retention endured 10×10^6 cycles of bending at a moment of 1,500 in.-lb and a steady centrifugal load of 31,500 lb. Visual inspection of the internal and external surfaces of the tube, butt face composite ends and surface and braze fillet shank end, prior to the first level revealed separations and delaminations as shown in Figures 25, 28 and 31. At the second fatigue level the spar and retention completed 10×10^6 cycles of 3,000 in.-lb bending with a 31,500 lb centrifugal load. Post-test visual inspection of the spars showed no indications of distress beyond

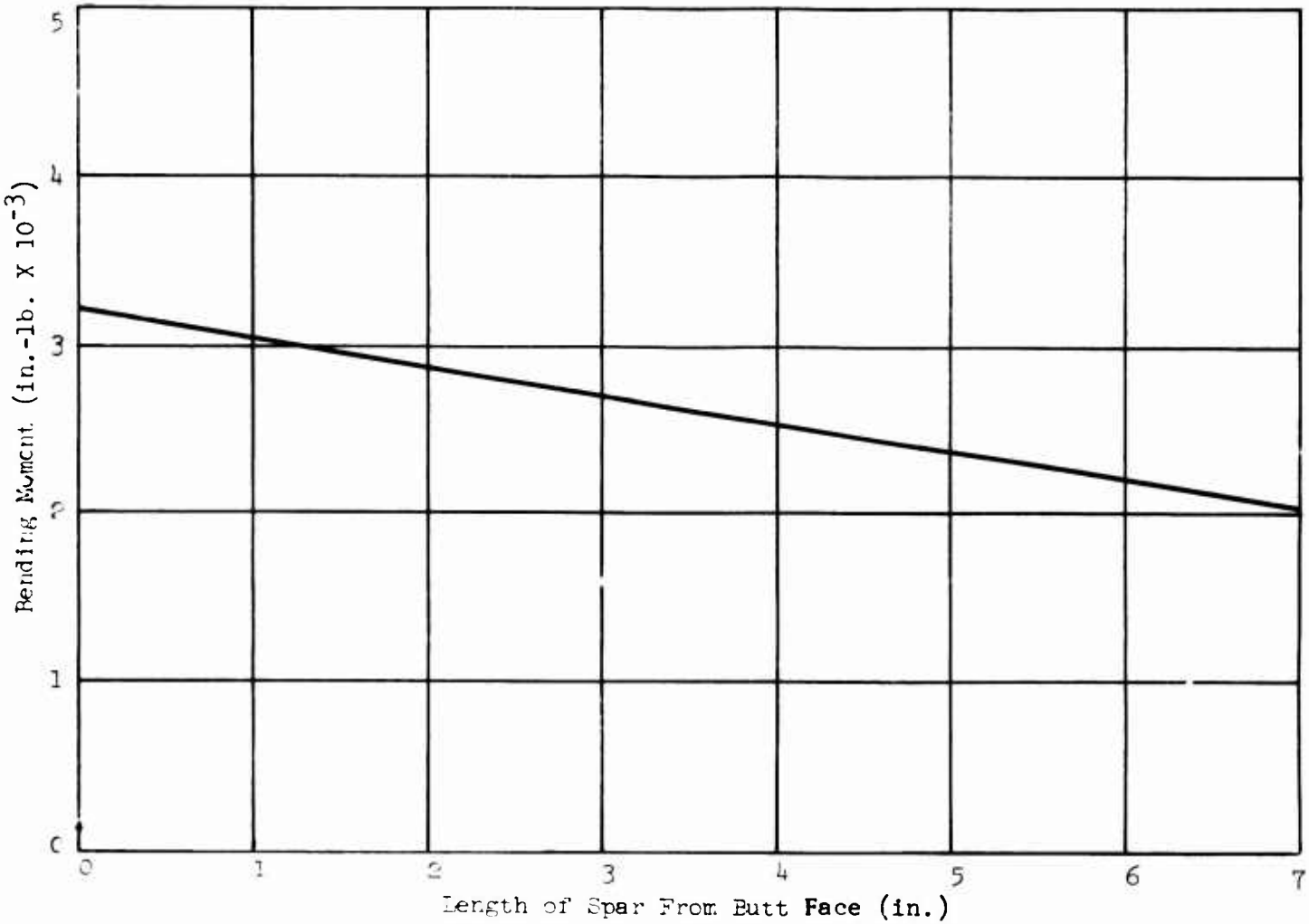

Figure 24. ESA (Static) Spar Moment Distribution.

TABLE II. BORSIC/ALUMINUM BLADE SPAR STRESSING

Test Bar	FBF Station	Gage Data: Direct.	Surf.	Coord.	No.	Centrifugal Load (lb): 7,800 lb	15,500 lb	23,500 lb	30,900 lb	1P-OOP*: 1,500 in.-lb	2,995 in.-lb	4,460 in.-lb
1	4.5	Long.	In	0°	2	4,640	9,040	13,310	17,540	- 790	-2,010	-3,030
		Hoop	In	0°	3	- 720	-1,217	-1,690	-2,150	- 272	- 360	- 580
		Long.	In	90°	6	3,870	8,220	12,650	17,230	270	290	460
		Hoop	In	90°	7	- 108	- 588	-1,085	1,630	128	96	144
		Long.	In	180°	11	4,440	8,880	13,390	18,120	1,490	2,510	3,920
		Long.	Out	0°	101	5,080	9,880	14,600	19,210	-1,070	-2,440	-3,790
		Hoop	Out	0°	102	- 220	- 636	-1,080	-1,570	204	236	388
		Long.	Out	90°	108	3,910	8,370	12,930	17,630	520	410	390
		Hoop	Out	90°	109	- 688	-1,440	-1,835	-1,642	152	160	276
		Long.	Out	180°	113	4,320	8,860	13,530	18,430	1,570	2,800	4,210
		Long.	Out	270°	118	4,310	9,010	13,710	18,560	350	310	580
2	4.5	Long.	Out	0°	201	4,050	8,540	13,130	17,530	- 990	-2,360	-3,390
		Long.	Out	90°	206	4,120	8,480	12,910	17,540	360	430	730
		Long.	Out	180°	209	5,470	10,230	15,080	19,610	1,670	3,150	4,530
		Long.	Out	270°	214	3,800	8,000	12,280	15,800	140	- 30	20
3	4.5	Long.	Out	0°	301	4,500	9,200	13,940	18,400	-1,100	-2,300	-3,640
		Long.	Out	90°	306	4,200	8,480	12,800	16,800	220	- 50	- 120
		Long.	Out	180°	309	4,640	9,220	13,800	18,080	1,610	3,000	4,600
		Long.	Out	270°	314	4,810	9,250	13,790	17,870	830	1,210	1,740
1	5.5	Long.	In	0°	4	4,830	9,600	14,360	19,020	- 980	-2,080	-3,130
		Hoop	In	0°	5	- 716	-1,235	-1,695	-2,190	272	368	584
		Long.	In	90°	8	4,190	8,710	13,350	18,090	260	280	480
		Hoop	In	90°	9	- 112	- 560	- 992	-1,505	116	52	136
		Long.	In	180°	12	4,210	8,770	13,420	18,290	1,400	2,460	3,650
		Long.	Out	0°	103	5,280	10,740	15,840	21,000	1,200	2,760	4,050
		Long.	Out	90°	110	4,320	9,510	14,400	19,620	-	-	-
		Long.	Out	180°	114	4,620	9,990	15,120	20,610	1,500	2,520	3,840
		Long.	Out	270°	119	4,680	10,170	15,300	20,790	-	-	-
2	5.5	Long.	Out	0°	202	4,680	10,110	15,210	20,250	1,110	2,730	3,930
		Long.	Out	90°	207	4,620	9,780	14,550	19,710	-	-	-
		Long.	Out	180°	210	5,640	11,190	16,500	21,510	1,500	2,700	3,930
		Long.	Out	270°	215	4,560	9,750	14,580	18,900	-	-	-
3	5.5	Long.	Out	0°	302	4,860	10,230	15,300	20,220	1,200	2,580	3,930
		Long.	Out	90°	307	4,650	9,780	14,670	19,290	-	-	-
		Long.	Out	180°	310	5,160	10,560	15,630	20,520	1,500	2,700	4,140
		Long.	Out	270°	315	4,980	10,170	15,000	19,620	-	-	-
1	7.0	Long.	Out	0°	105	4,990	9,820	14,770	19,560	- 980	-2,320	-3,260
		Long.	Out	180°	115	4,280	9,070	14,010	19,100	1,480	2,600	4,150
2	7.0	Long.	Out	0°	203	4,620	9,430	14,370	19,050	- 960	-2,180	-3,120
		Long.	Out	180°	211	5,240	10,130	15,160	19,820	1,480	2,670	4,120
3	7.0	Long.	Out	0°	303	4,410	9,220	14,060	18,560	-1,060	-2,180	-3,230
		Long.	Out	180°	311	4,790	9,570	14,390	18,870	1,510	2,810	4,370
1	8.5	Long.	Out	0°	106	4,600	9,480	14,540	19,500	- 880	-2,030	-2,900
		Long.	Out	180°	116	4,410	9,320	14,430	19,670	1,470	2,470	3,880
2	8.5	Long.	Out	0°	204	4,570	9,450	14,460	19,180	- 860	-2,000	-2,790
		Long.	Out	180°	212	5,020	9,890	14,950	19,620	-1,420	-2,500	-3,800
3	8.5	Long.	Out	0°	304	4,440	9,340	14,290	18,880	- 880	-1,990	-3,020
		Long.	Out	180°	312	5,060	9,960	14,930	19,520	1,540	2,720	4,090

*At 5.5" from butt face (FBF)

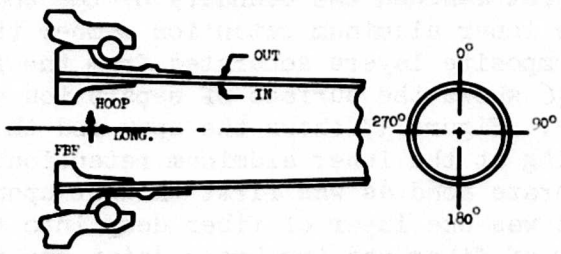

that noticed during the original inspection. The bars were then reassembled for fatigue testing at the third level of 4,500 in.-lb bending moment and 31,500 lb centrifugal load. After 3.6×10^6 cycles at the third level, the test was shut down by automatic control. Upon restarting, it was noted that the frequency was down approximately 1.5 Hz. An external inspection of the assembly revealed that the separation of the braze joint at the retention, spar interface on arms 1 and 2 had grown substantially, as shown in Figures 26, 29 and 32. At this point, it was decided to continue the testing at the 4,500 in.-lb moment level, until fracture or 10×10^6 cycles. At the completion of 10×10^6 cycles, the barrel was completely disassembled and inspected.

The post-test inspection revealed that the cracking at the retention end had not grown significantly from the condition observed after 3.6×10^6 cycles at the third test level (see Figures 27, 30 and 33). The retention system was completely disassembled at this time and visually inspected. The inspection showed the area at the bond line between the composite and the inner aluminum retention member to be cracked on nearly 100% of the circumference of the butt face of all three spars. See Figure 34. The inspection also showed a severe delamination and buckling of the composite over 90 degrees of the circumference at the outboard end of the inner retention member on spar number three. See Figure 35. The spars were not disassembled and inspected at 3.6×10^6 cycles of the third test level, however, it is believed that the fractures occurred at this point because of the significant frequency change noted when the vibration motor shut the test down via automatic control at this point in the cycling. Such a frequency change is usually the sign of a fracture. The severe buckling and delamination shown in one spar is believed to have occurred due to the continued cycling beyond fracture with a loading distribution changed significantly due to the fracture.

Spar number three was then used for a destructive examination of the retention. The destructive examination showed the inner aluminum retention member to be completely detached from the composite material. Figure 36 shows the section of the retention which was removed. The sectioning cut was not completed because as the depth of cut reached the boundary of the composite material and the inner aluminum retention member the outer retention and composite layers separated from the inner aluminum layer. Figure 36 shows the surface of separation when looking at the composite. Figure 37 shows the spar and the surface of separation looking at the inner aluminum retention. The fracture was not in the braze bond as was first thought upon visual examination, but was one layer of fiber deep into the composite. The single layer of fiber and the braze joint can be clearly

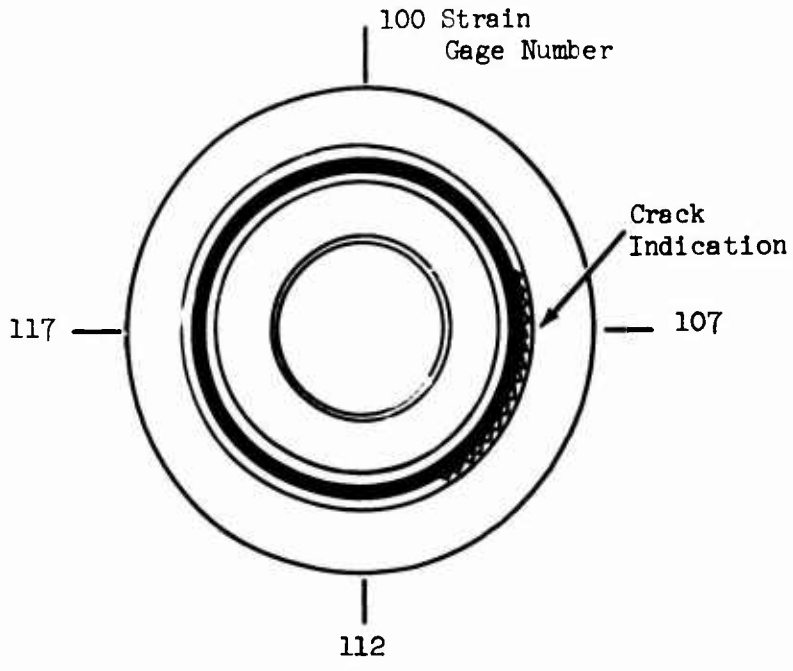

Figure 25. Schematic of Retention Indications of Spar Number 1 Prior to FSI.

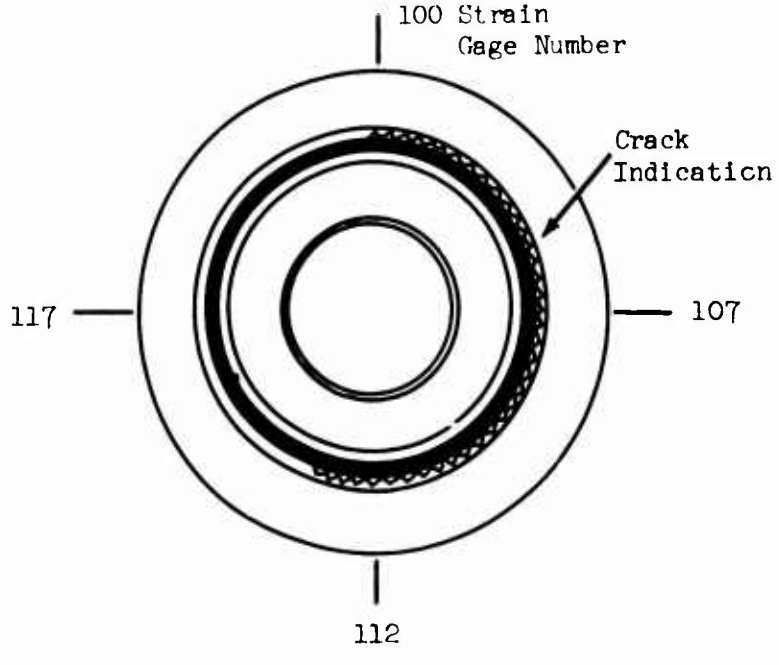

Figure 26. Schematic of Retention Indications of Spar Number 1 After FSI.

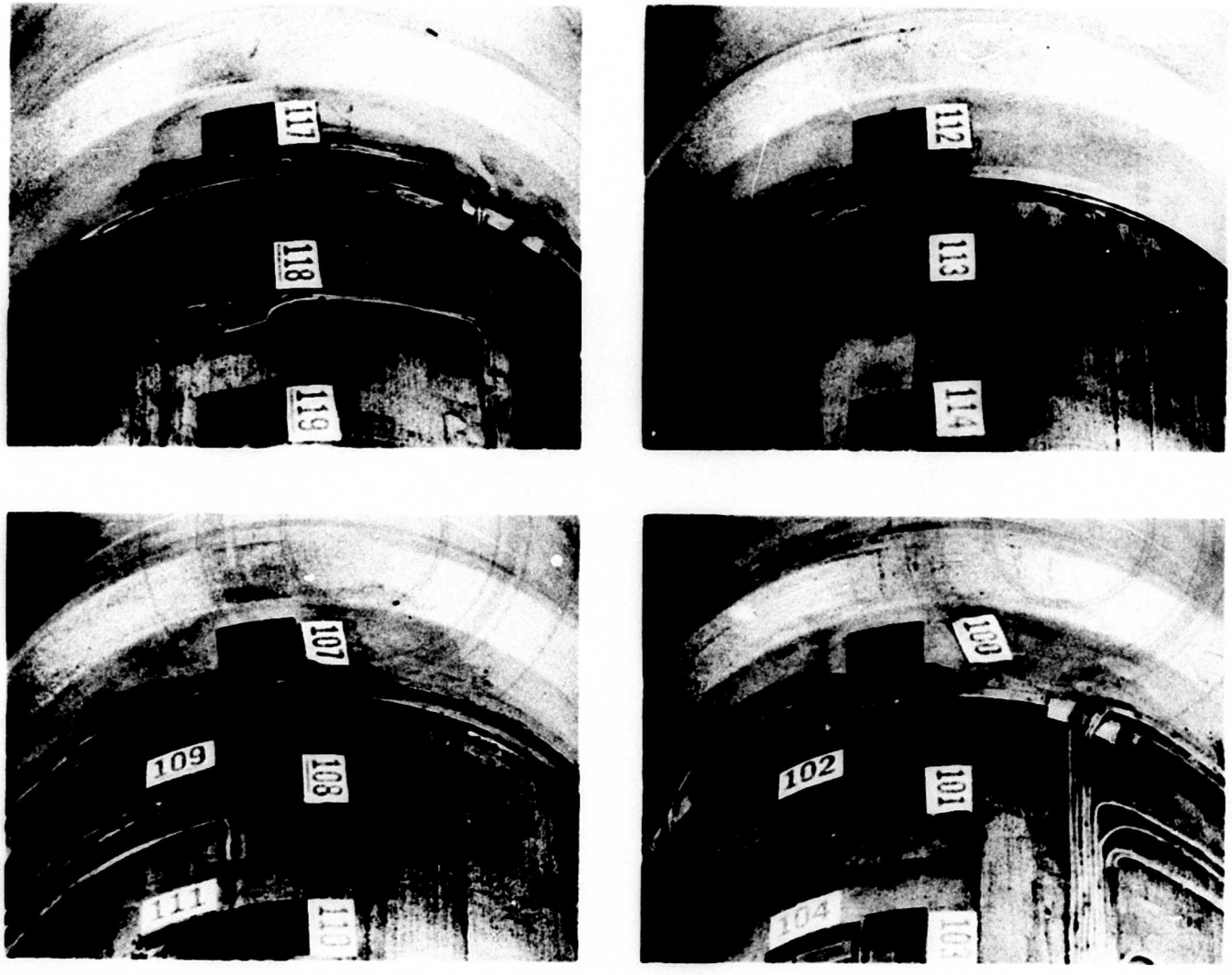

Figure 27. Outer Retention Ending of Spar Number 1 After FSI.

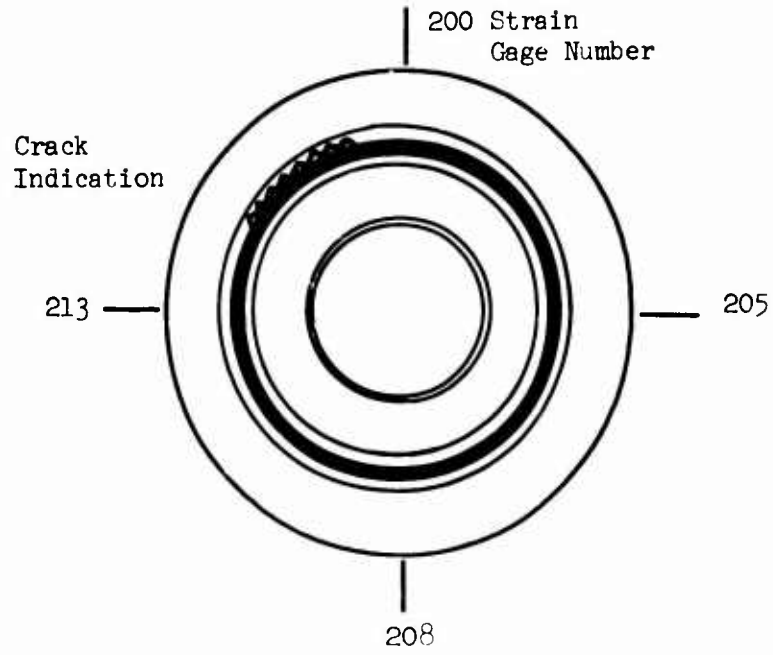

Figure 28. Schematic of Retention Indications of Spar Number 2 Prior to FSI.

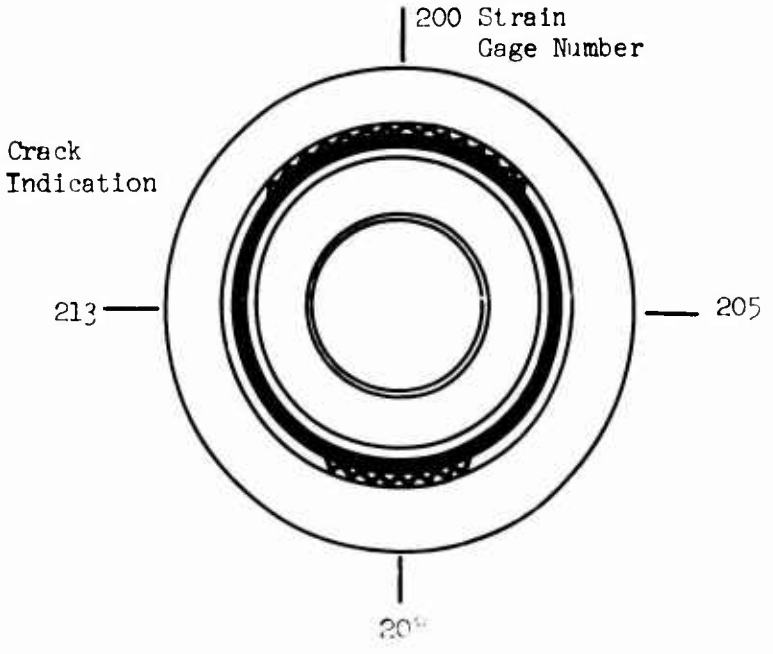

Figure 29. Schematic of Retention Indications of Spar Number 2 After FSI.

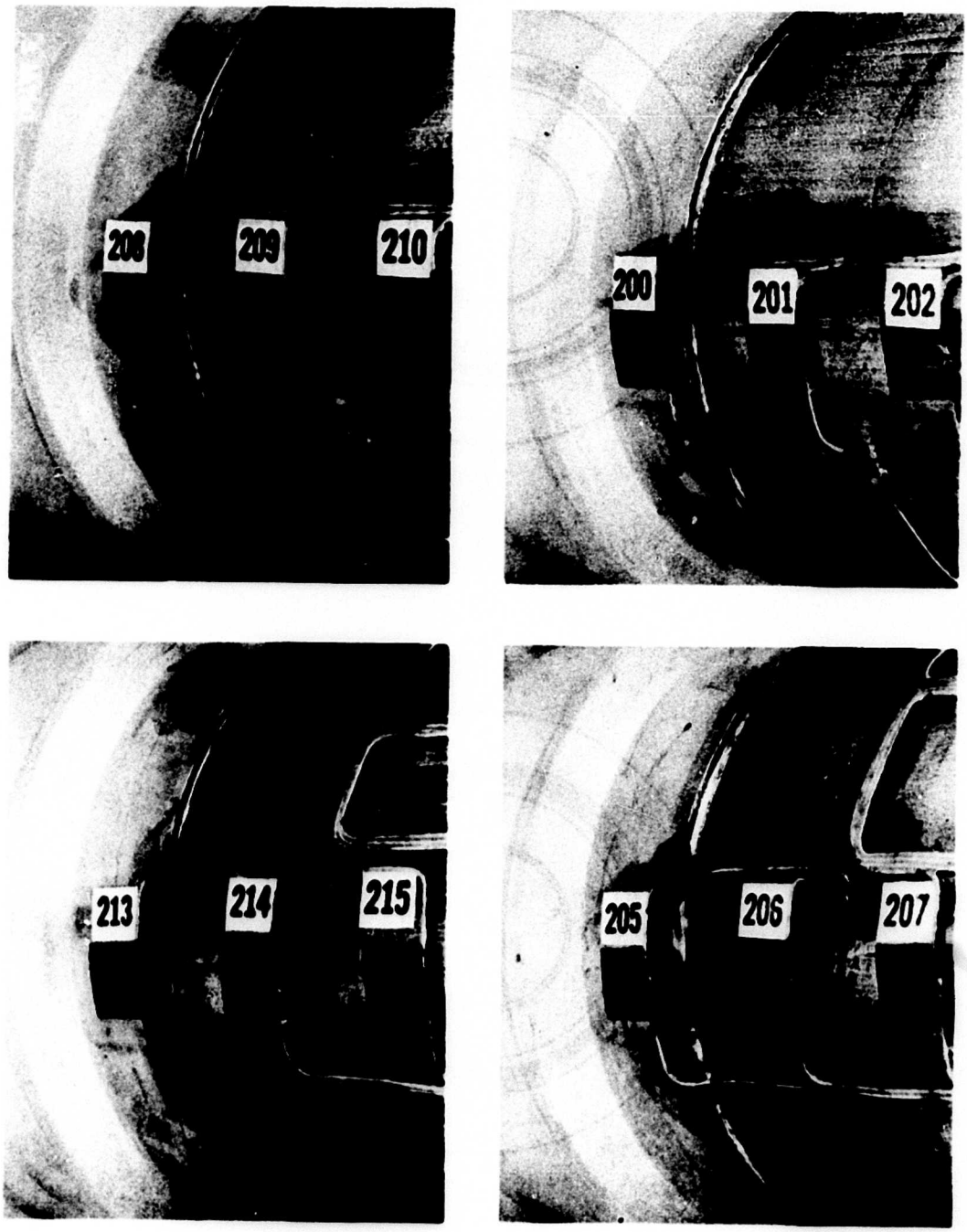

Figure 30. Outer Retention Ending of Spar Number 2 After FSI.

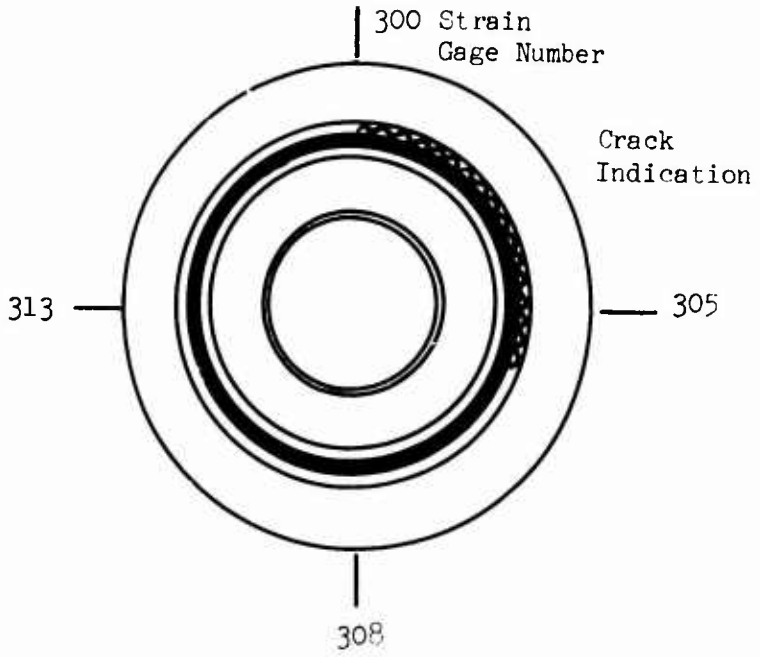

Figure 31. Schematic of Retention Indications of Spar Number 3 Prior to FSI.

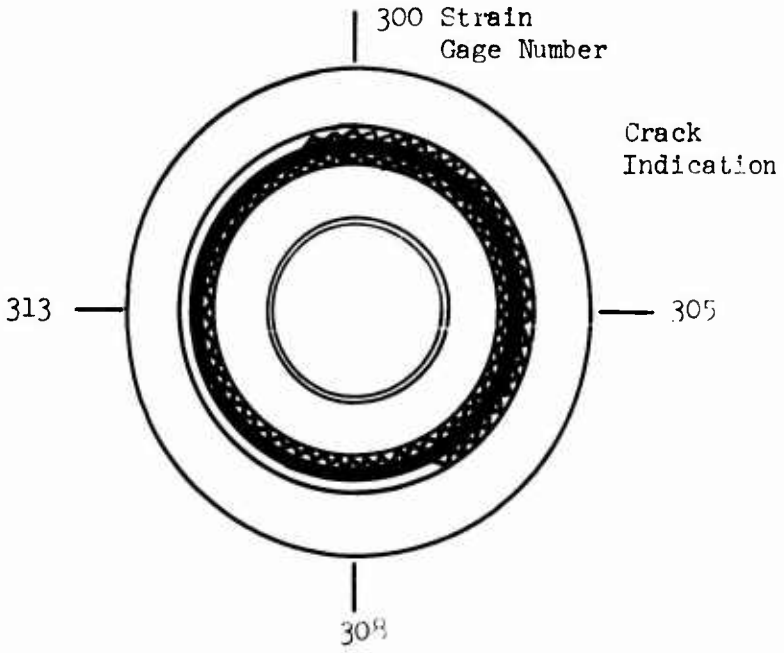

Figure 32. Schematic of Retention Indications of Spar Number 3 After FSI.

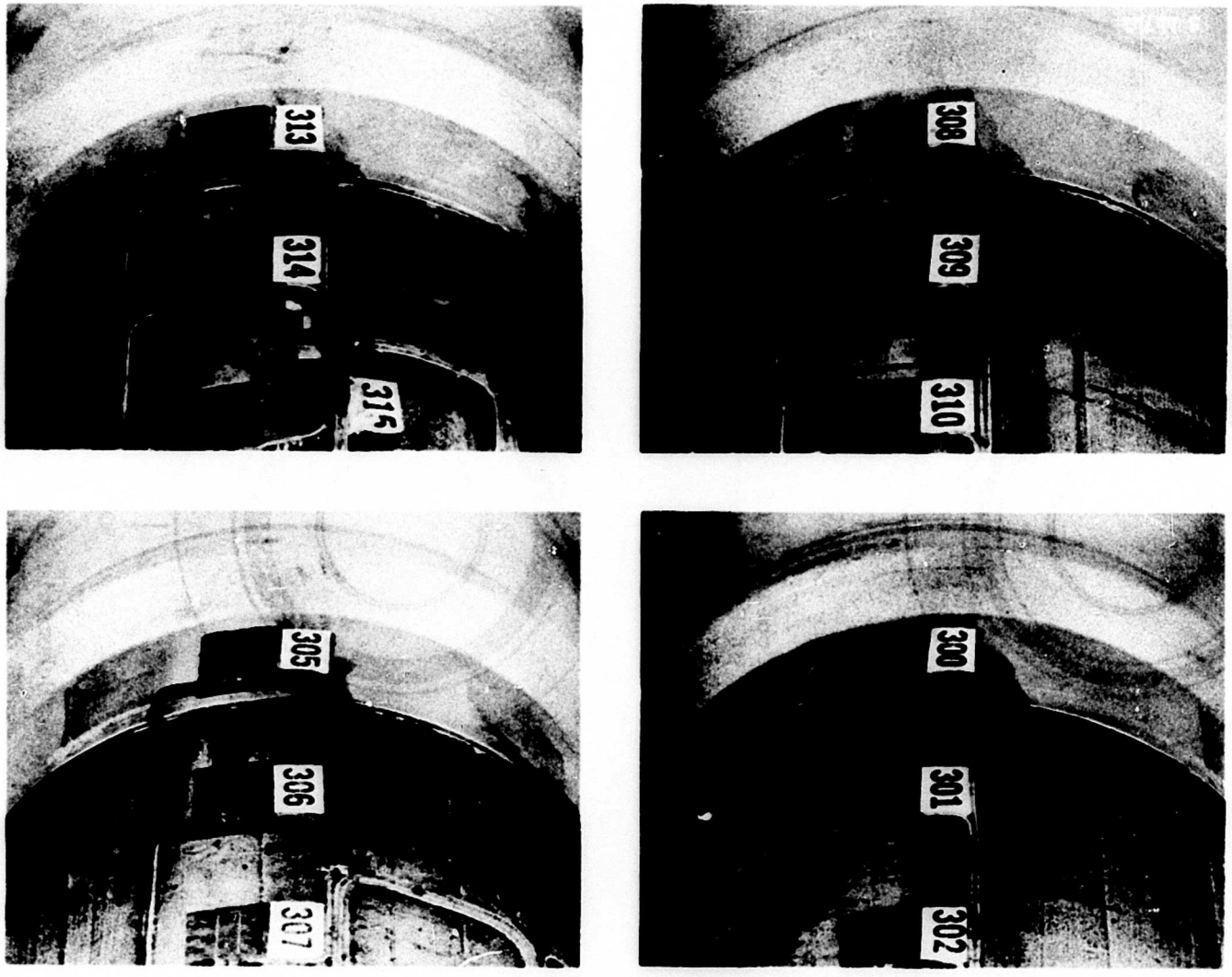

Figure 33. Outer Retention Ending of Spar Number 3 After FSI.

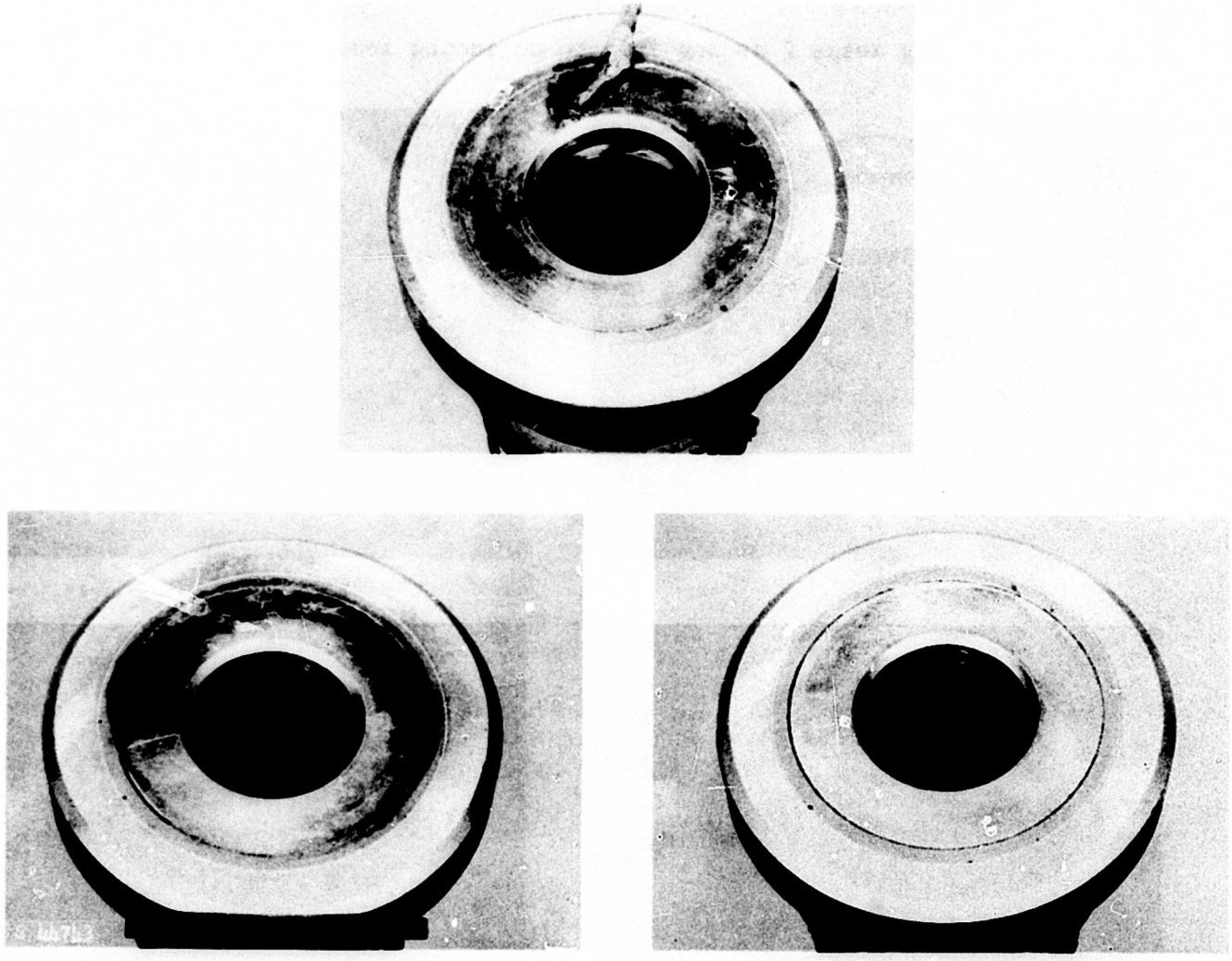

Figure 34. Butt Faces of Spars After FSI.

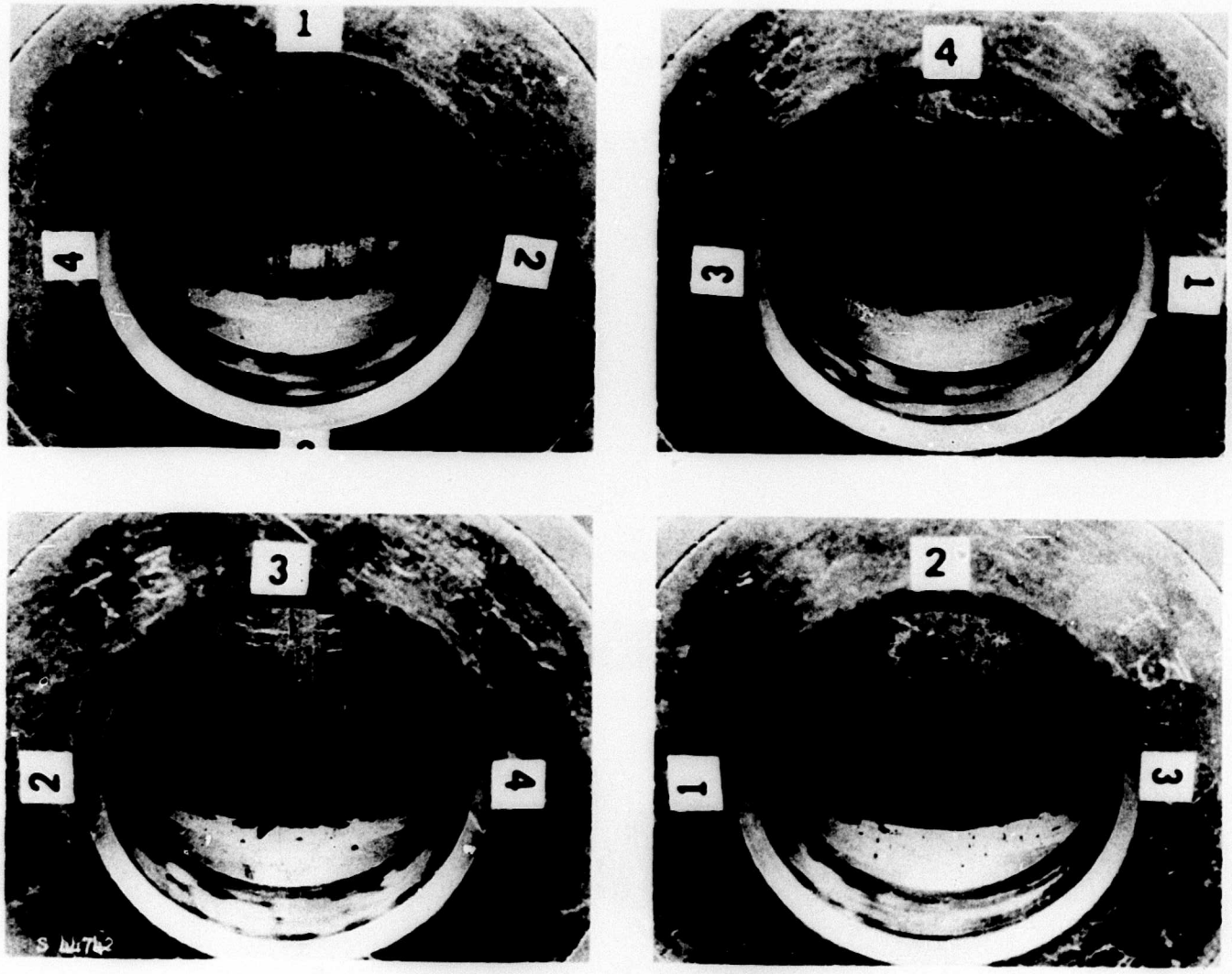

Figure 35. Inner Retention of Spar Number 3 After FSI.

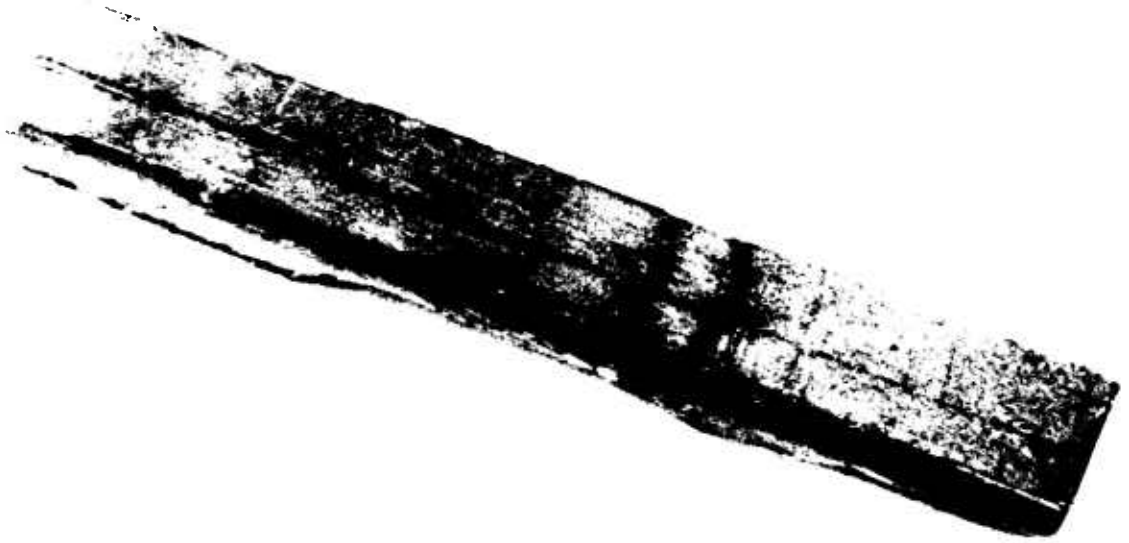

Figure 36. Retention Segment for Post-Test Evaluation, Spar Number 3.

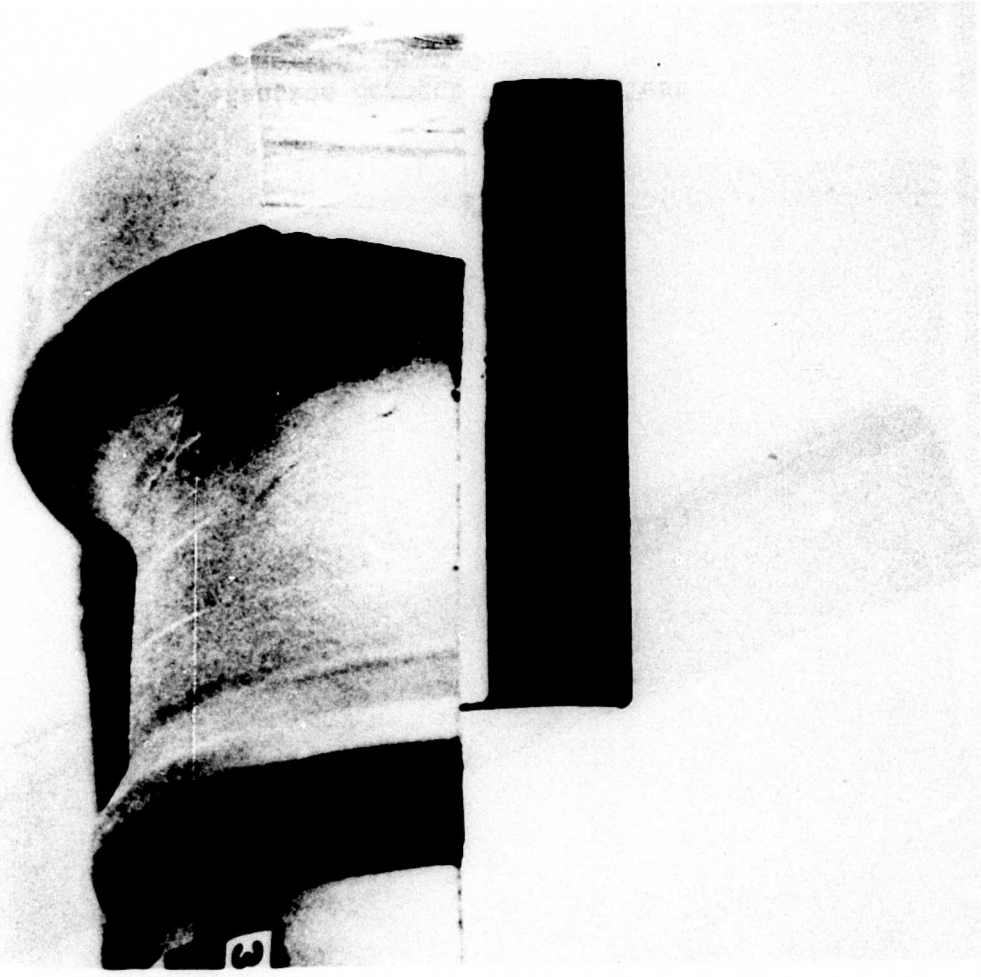

Figure 37. Spar Area From Which Segment Was Removed.

seen in the micro-section of the inner retention member shown in Figure 38. The fracture is a failure of the fiber-to-matrix bond as can be seen by the perfectly clean appearance of the fiber layer left attached to the inner retention as shown in Figure 39. This is typical of the fracture around the entire circumference of the inner retention member on spar number three.

A second spar from the fatigue test was sectioned, and damage of a similar nature to that on spar number three was found. The degree of the damage was not as severe on the second spar examined. The outer retention to composite joint appeared to be sound nearly all the way around the circumference. The inner retention was pulled away from the composite at both the butt face and the retention end. The separation was, again, not in the braze area, but one fiber layer deep into the composite. The separation was over the entire circumference on both ends of the retention and approximately one inch long from either end.

Photomicrographs were made of the fractured areas and may be seen in Figures 38, 39 and 40. Figure 38 shows the bond area of the inner retention member of spar number 3. The retention, braze joint, fiber and matrix may all be seen clearly in this photomicrograph. As has been stated, the fracture is a fiber-to-matrix delamination in the first layer of the composite. The braze joint was solid and intact throughout. Figure 39 shows the bond area between the composite and the outer retention member. Here the braze joint appears to have separated and in one area, over the width of two fibers, the braze apparently did not wet the composite surface at all. Figure 40 shows the outer retention bond area on an untested spar. This area was chosen because a crack at the braze joint was noticed. This area is then a direct comparison with that of the outer retention on the tested spar. The untested spar photomicrograph clearly shows that the braze did not wet the composite during the manufacturing operation.

The fractures found in the BORSIC/Al spar retention areas are typical of fractures generated by repeated bending in test specimens as well as actual design configurations. The fractures indicate that the weak link in the braze, matrix and fiber system is the matrix-to-fiber bond. The stress values obtained in actual testing and the fatigue endurance of the spars show the design values for shear fatigue limit to be reasonably accurate.

A comparison of the design calculated values for stress in the spars and the actual stress measured in the spars shows the two to be in agreement. Figures 41 and 42 show the stress levels

COMPOSITE

ONE LAYER OF COMPOSITE
BRAZE AND INNER ALUMINUM
SUPPORT

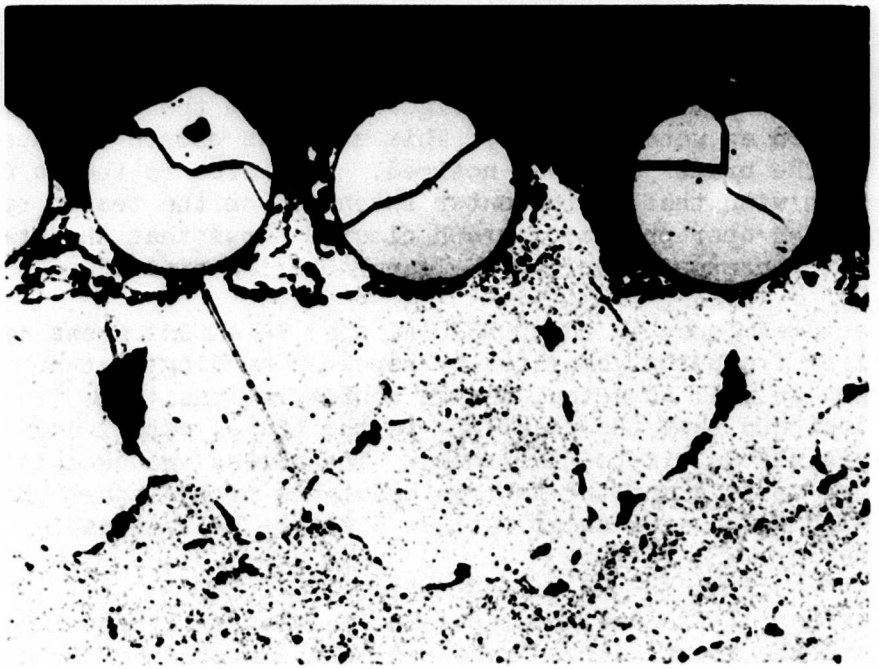

Figure 38. Photomicrographs of Inner Retention Bond Area, Spar Number 3.

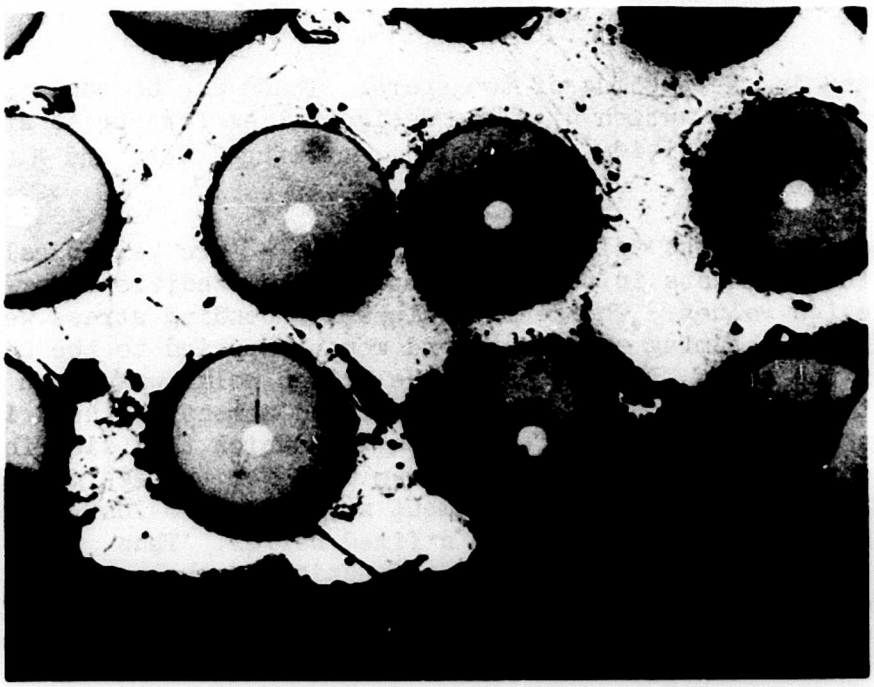

COMPOSITE

OUTER ALUMINUM
RETENTION

Figure 39. Photomicrographs of Outer Retention Bond Area, Spar Number 3.

obtained in the testing of the spars. These can be compared with Figures 6 and 7, which give the design values for stress at the same loading condition (31,500 lb centrifugal load and 3,000 in.-lb bending moment).

The bending stress values shown in Figure 42 are values calculated from the test data in order to compare like conditions for test and design values. The design values for bending stress were calculated assuming a constant end moment applied to the outboard end of the spar. In this case, the design point was at an end moment of 3,000 in.-lb. The constant end moment was used in the design analysis because of the ease with which this distribution can be put into the computer program used for the design. It is more practical from an equipment standpoint to load the spars in bending by an end load with a fixed barrel. Thus, the strain values measured in the test are a function of the moment distribution shown in Figure 24. In order to compare the test values with the design calculated values the test values must be modified by the following equation.

$$\sigma_{3000} = \sigma_{\text{actual}} \left(\frac{M_{3000}}{M_{\text{actual}}}\right)$$

Thus, by knowing the moment distribution and the actual stress at any point in the distribution the stress due to a 3,000 in.-lb moment at that point can be calculated. This equation was used to generate the curve on Figure 42 for comparison with the design values in Figure 7.

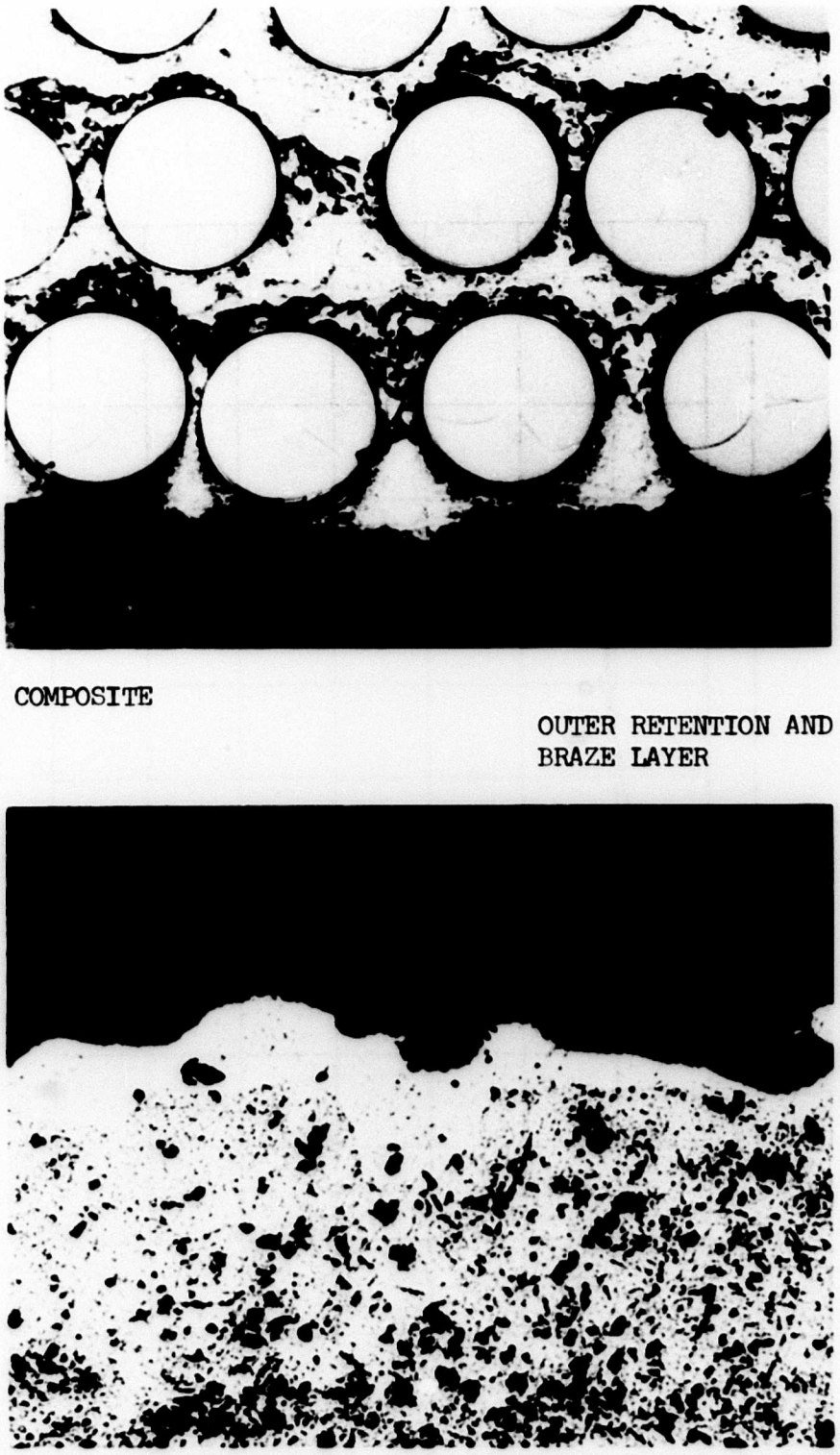

Figure 40. Photomicrographs of Outer Retention Bond Area on Untested Spar.

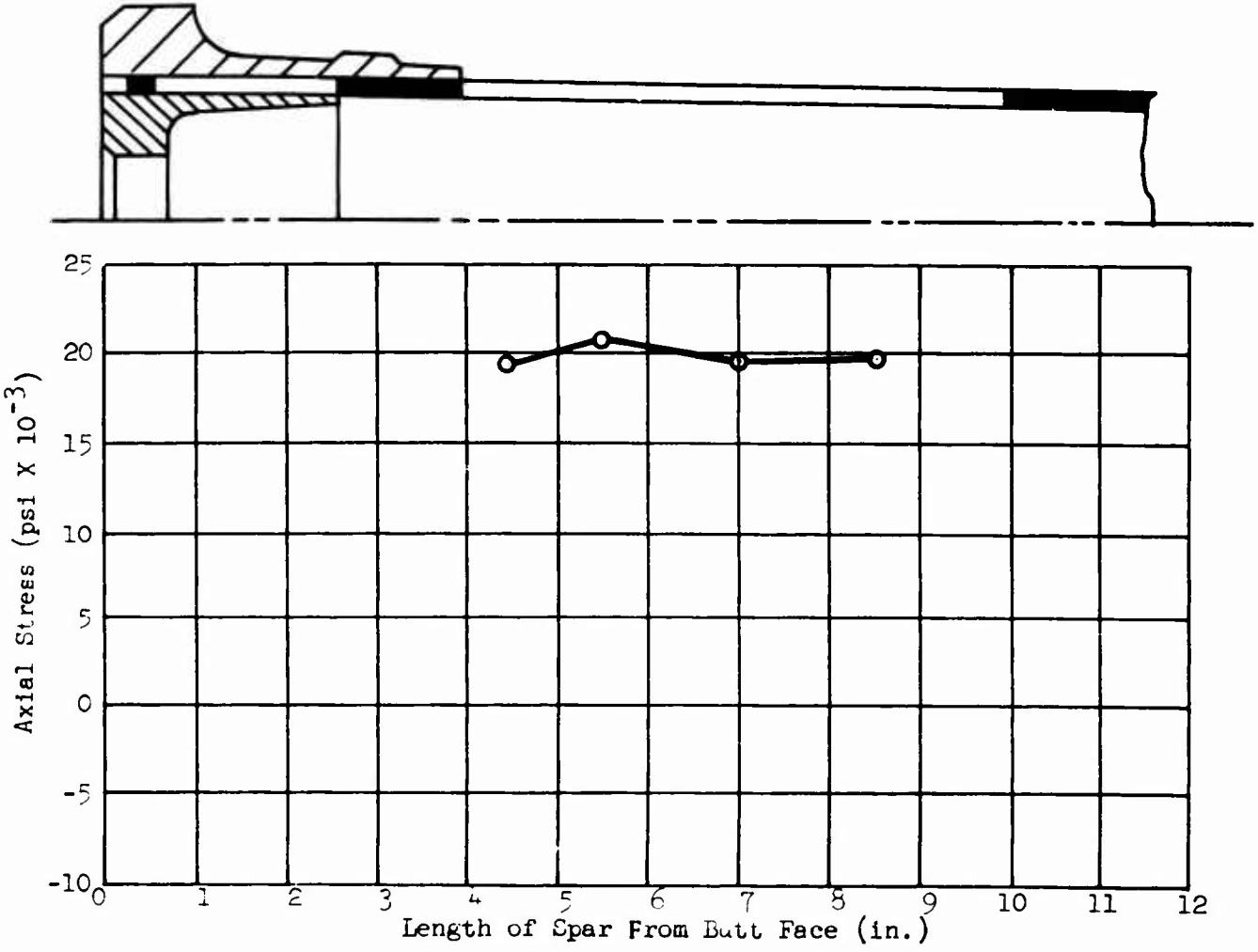

Figure 41. ESA Axial Stress.

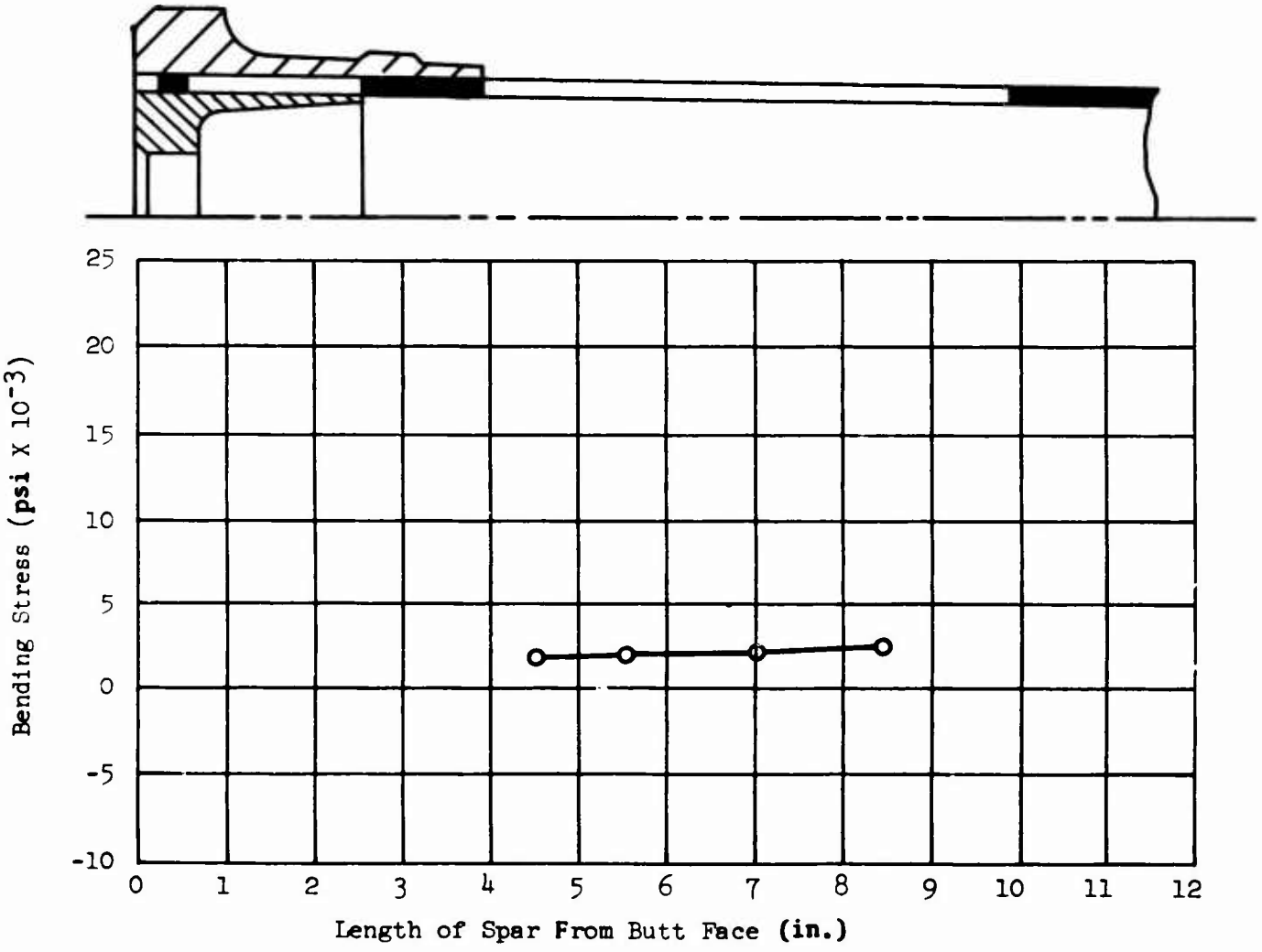

Figure 42. ESA Bending Stress.

CONCLUSIONS

The retention system performed as expected during the ESA (static) and FSI (fatigue) phases of testing. The stress values obtained during testing agreed with the calculated values.

The failure of the retention occurred after 3.6×10^6 cycles of bending at 4,500 in.-lb moment and a steady centrifugal load of 31,500 lb. This failure occurred after the specimen had also accumulated 10×10^6 cycles of bending moment at 1,500 in.-lb and 10×10^6 cycles of bending at 3,000 in.-lb, each with 31,500 lb centrifugal load. The design condition was 10×10^6 cycles at 3,000 in.-lb and 31,500 lb centrifugal load.

The failure mode was a fiber-to-matrix debond one layer deep into the composite material in the retention area. The failure was initiated by a transverse crack at the inner retention ending.

The outer retention exhibited some voided areas in the braze joint due to manufacturing techniques. These areas were only slightly affected by fatigue damage.

In view of these conclusions, it is evident that a full-size retention can be designed and manufactured with minor modifications made to accommodate the larger size of the full-scale hardware.

RECOMMENDATIONS

In view of the encouraging results obtained from this program, it is recommended that a continuing development program be pursued which would be directed toward the ultimate goal of producing a full-size propeller blade utilizing a composite spar. To attain this goal, four general development steps are deemed necessary:

1. The design, fabrication and fatigue test of a full-size retention to further enhance the design as well as fabrication techniques.

2. Fabrication studies to determine the forming feasibility of full-size spar sections outboard of the retention area of the spar.

3. The design, fabrication, and fatigue test of the formed spar outboard of the retention area to acquire essential data to further enhance design and fabrication technique.

4. The design and fabrication of full-size blades employing a composite spar for engine whirl tests.

Item 1 appears to be the next logical step; however, due to the lead time required to develop the process of forming full-size spar sections outboard of the retention area, consideration should be given to implementing item 2 in conjunction with item 1.

LITERATURE CITED

1. Currie, D. P., DETAILED DESIGN OF A 2000-SHP ADVANCED TECHNOLOGY V/STOL PROPELLER SYSTEM, Hamilton Standard Div., United Aircraft Corp.; USAAVLABS Technical Report 69-59, U. S. Army Aviation Materiel Laboratories, Fort Eustis, Virginia, AD864446.

2. Kalinis, A., ANALYSIS OF SHELLS OF REVOLUTION SUBJECTED TO SYMMETRICAL AND NON-SYMMETRICAL LOADS, Journal of Applied Mechanics, September 1964.

APPENDIX

HAMILTON STANDARD PLAN OF TEST

JOB: BORSIC^{R}/Aluminum Blade Shank Evaluation

PLAN PREPARED BY: J. L. Mattavi

PROJECT & ORDER:

APPROVED BY: G. Molter

INSTRUCTION:

TEST ENGINEER:

TIME PERIOD: TO:

1. WHAT IS ITEM BEING TESTED?
2. WHY IS TEST BEING RUN? WHAT WILL RESULTS SHOW OR BE USED FOR?
3. DESCRIBE TEST SETUP, INCLUDING INSTRUMENTATION. ATTACH SKETCH OF INSTALLATION.
4. ITEMIZE RUNS TO BE MADE GIVING, LENGTH OF EACH AND READINGS TO BE TAKEN.
5. SPECIAL INSTRUCTIONS: SAFETY PRECAUTIONS FOR OPERATORS AND HANDLING EQUIPMENT. OBSERVATIONS BY SIGHT, FEEL, OR HEARING. LIST POINTS OF OBSERVATION WHICH MIGHT CONTRIBUTE TO ANALYSIS OF (A) PERFORMANCE OF UNITS, (B) INCIPIENT TROUBLE BEFORE IT OCCURS, AND (C) CAUSE OF FAILURE.
6. HOW WILL DATA BE USED OR FINALLY PRESENTED? GIVE SAMPLE PLOT, CURVE, OR TABULATION AS IT WILL BE FINALLY PRESENTED.

NUMBER ENTRY AS LISTED ABOVE AND DESCRIBE BELOW

1. BORSIC/Aluminum Blade Shank, P/N 159X-95, exhibiting 33LF shank geometry.

2. The subject shank design will be subjected to an experimental stress analysis (ESA) and fatigue strength investigation (FSI) to determine the structural characteristics of BORSIC/Aluminum configured into a proven blade shank design.

3. The test setup is composed of three test bars manufactured from BORSIC/Aluminum in the shank area assembled into an existing 33LF barrel. Loading will consist of a simulated centrifugal load and a bending moment. The axial (simulated centrifugal) load is provided by an internal wedge mechanism. The bending moment is applied statically for the ESA by pulling on the end of the test bar with a calibrated cable-spring combination, and dynamically for the FSI by vibrating the bars at their first natural frequency. Load measurement will be supplemented by strain gages mounted along the test bars. Figure 43 illustrates the barrel assembly and loading directions.

4. Testing will consist of two phases corresponding to the ESA and FSI aspects respectively. In preparation for the ESA, strain gages will be placed at suspected areas of highest stressing. See Figure 44. The gage locations indicated in Figure 44 by a small circle (o) will be covered on all three shanks. The remaining gages will be applied to one shank only. Since all three test bars exhibit the same configuration, the extensively gaged bar will yield stress magnitude and distribution values for this configuration. The additional gages on the remaining bars will be used to assure proper 3P loading during the subsequent FSI and will also indicate geometric variations resulting from manufacturing tolerances. Centrifugal loading will be applied in increments of the limit load and load and strains recorded. With a percentage of limit load on the test bars, bending moment will be incrementally applied and strains recorded. Upon completion of this loading phase, the barrel will be disassembled and the test bars inspected for indications of distress.

   In preparation for the FSI phase, the barrel will be reassembled for testing in the 3P-OOP mode. 3P indicates that all three arms are vibrating in phase with each other, and OOP indicates that the direction of vibration is "out-of-the-plane" of rotation.

Testing will be conducted at the three levels contained in Table III at a design frequency of 82 hertz. Test level duration will be 10 X 10^6 cycles or fracture, whichever occurs first. At the completion of each level, the barrel will be disassembled and the test bars examined for signs of distress.

Before cycle testing is initiated, the barrel assembly will be tuned to yield equal shank stress values among the three bars. The moment level will then be determined as a function of strain gage readings of the test bars. Selected strain gages will be used to monitor the cyclic moment during testing. In addition to these strain gage readings, the rate of cycling, number of cycles, test time, date, and time of day will be recorded periodically during testing.

If any or all of the test specimens described above survive the three levels of fatigue testing, they will be inspected and tensile tested to determine their residual tensile strength. Testing will be conducted as in the Phase II program (Contract DAAJ02-68-C-0079), using the Baldwin-Southwark 200,000-lb. tensile machine.

5. During fatigue testing, the frequency will be examined regularly to detect any incipient malfunctions. Fracture of a major component will be indicated by a marked difference in frequency or gage readings. During testing, the barrel will be filled with MIL-L-7808 oil which will be examined periodically for fretting indications which would show up as dirt particles in the oil.

6. The testing data will be analyzed and presented in a Hamilton Standard External Report.

TABLE III. 3P OUT-OF-PLANE (OOP) FATIGUE TESTING OF BORSIC/ALUMINUM BLADE SHANKS

Level	Cyclic 3P-OOP* Bending Moment (in.-lb)	Centrifugal Load (lb)	No. of Cycles** per level
1	1,500	31,000	10×10^6
2	3,000	31,000	10×10^6
3	4,500	31,000	10×10^6

*Moment per arm at retention.

**Or fracture, whichever comes first.

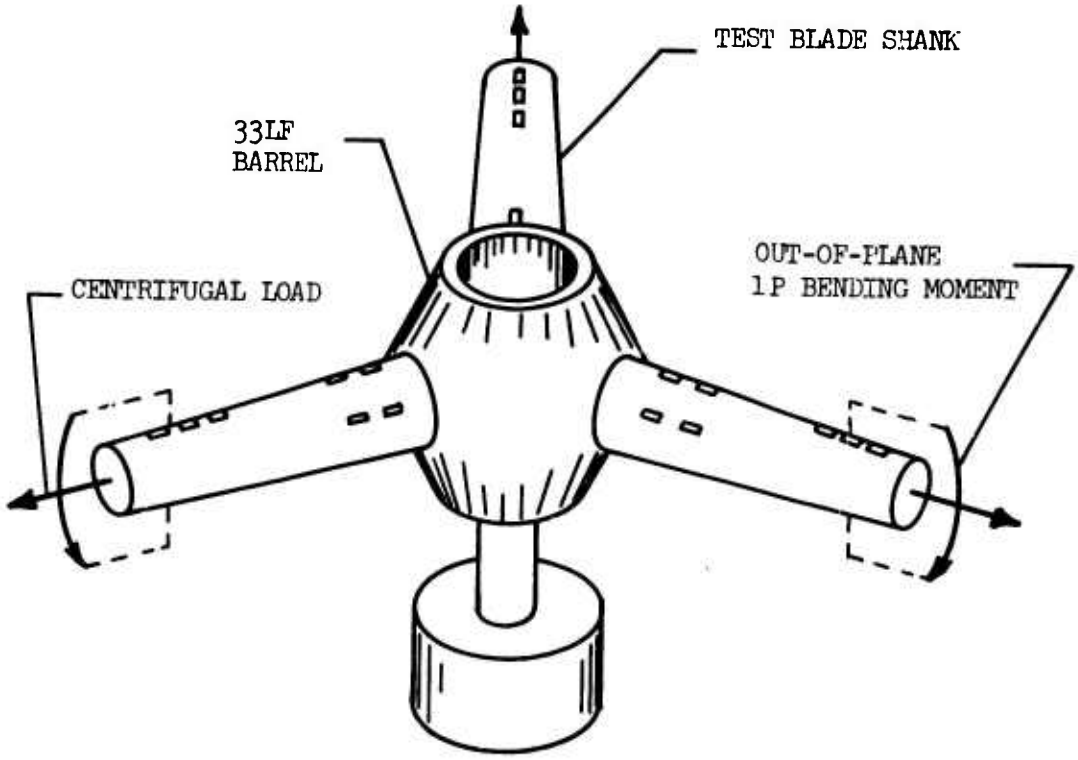

Figure 43. BORSIC/Aluminum Blade Retention Test Load Diagram.

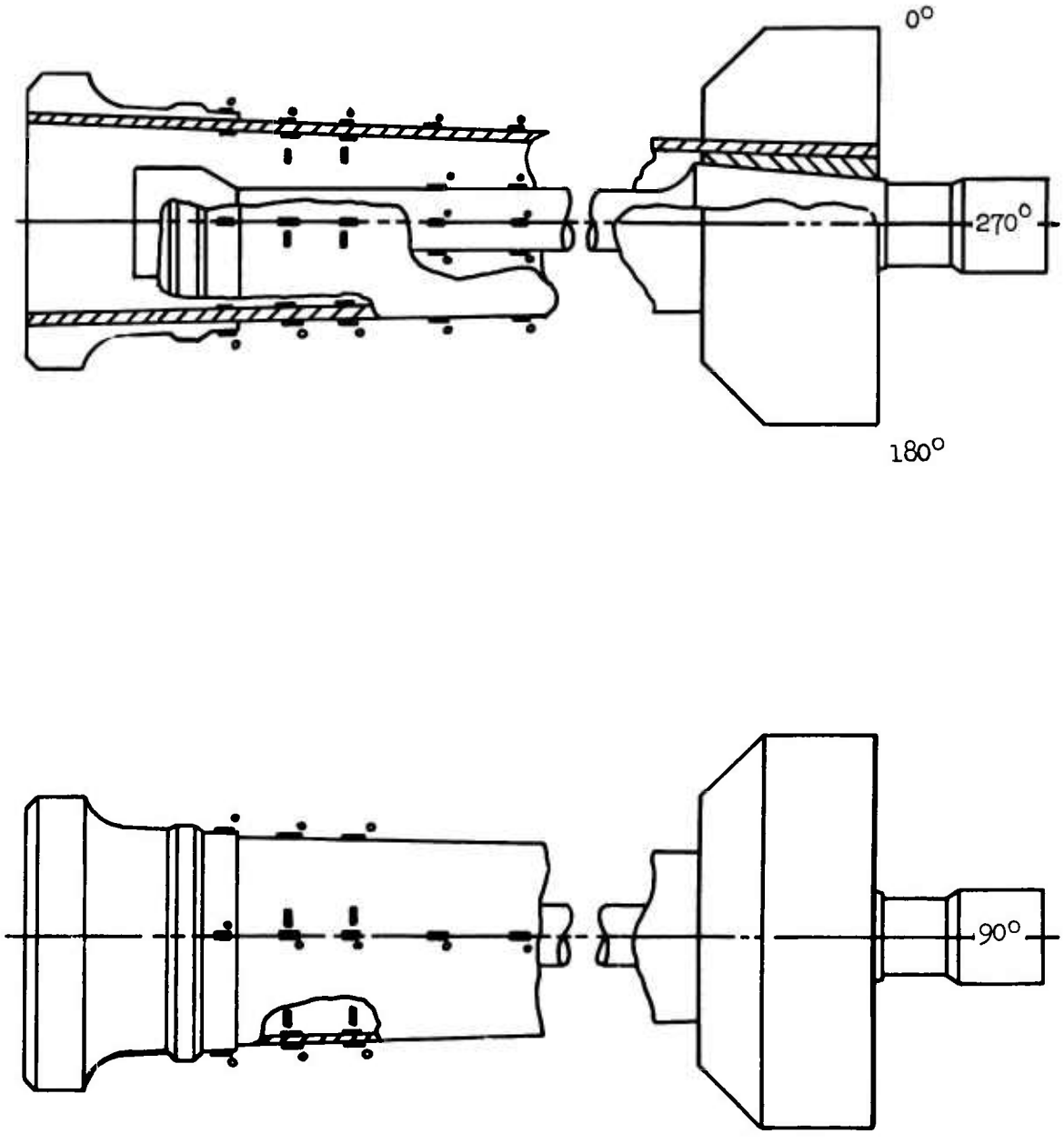

Figure 44. Strain Gage Locations for ESA and FSI.